# **Recent Results on Stability of Planar Detonations**

Kevin Zumbrun

Dedicated to Guy Métivier on the occasion of his 65th birthday.

**Abstract** We describe recent analytical and numerical results on stability and behavior of viscous and inviscid detonation waves obtained by dynamical systems/Evans function techniques like those used to study shock and reaction diffusion waves. In the first part, we give a broad description of viscous and inviscid results for 1D perturbations; in the second, we focus on inviscid high-frequency stability in multi-D and associated questions in turning point theory/WKB expansion.

In these notes, we describe some recent work on stability and behavior of detonation waves, carried out from a point of view evolving from the study of viscous and inviscid shock and boundary layers in, e.g., [11, 27, 29, 30, 33–36, 57, 68, 91–93]. This material was originally presented as a pair of 90-min lectures at the INDAM conference *Nonlinear Optics and Fluid Mechanics*, given in Rome, September 14–18, 2015 in honor of the 65th birthday of Guy Métivier, and our treatment follows closely to the spirit and format of the lectures.

The topic was chosen for interest of the honoree as almost the unique one studied by the author on which he has not explicitly collaborated with Métivier; nonetheless, many of the ideas may be seen to be related to ideas and tools developed by and with Guy in other contexts. The material presented here was developed in joint work with Blake Barker, Jeff Humperys, Olivier Lafitte, Greg Lyng, Reza Raoofi, Ben Texier, and Mark Williams. We mention also the foundational work of Kris Jenssen together with Lyng and Williams [40], of which we make frequent use.

Research of K.Z. was partially supported under NSF grants no. DMS-0300487 and DMS-0801745.

K. Zumbrun (⊠)

Department of Mathematics, Indiana University, 47405, Bloomington, IN, USA e-mail: kzumbrun@indiana.edu

## 1 Stability of Viscous and Inviscid Detonation Waves

In this first part, we survey a collection of theoretical and numerical results on *1D* stability of detonations obtained over the past 10–15 years via Evans function-based techniques like those used to study shock and reaction diffusion waves. These include stability in the small heat-release and high-overdrive limits, rigorous characterization of 1D instability as "galloping" type Hopf bifurcation, description of the inviscid (ZND) limit, and numerical computation of viscous (rNS) spectra revealing a new phenomenon of "viscous hyperstabilization."

Two underlying questions we have in mind in this section are:

- What is the (physical or mathematical) role of viscosity in the theory?
- What is our role in the theory? That is, what can we usefully contribute to the (physical or mathematical) study of detonations by the introduction of Evans function-based techniques?

## 1.1 Viscous and Inviscid Detonation Waves

Consider a general abstract combustion model with one-step reaction, expressed in 1D Lagrangian coordinates [53–55, 82, 91]:

$$v_t + f(v)_x = \varepsilon (B(v)v_x)_x + kq\phi(v)z,$$
  

$$z_t = \varepsilon (C(v, z)z_x)_x - k\phi(v)z,$$
(1)

 $v, f, q \in \mathbb{R}^n, B \in \mathbb{R}^{n \times n}, z, C, \phi, k, \varepsilon \in R^1$ , and  $k, \varepsilon > 0$ . Here, v comprises gas-dynamical variables, z = mass fraction of reactant,  $\phi(v) =$  "ignition function", q = heat release, k = reaction rate, and  $\varepsilon$  (typically small) scales coefficients of viscosity/heat conduction/species diffusion.

A right-going detonation solution consists of a traveling wave

$$(v,z)(x,t) = (\bar{v},\bar{z})(x-st), \qquad \lim_{x \to +\infty} (v,z)(x) = (v_{\pm},z_{\pm}),$$

s > 0, with  $z_- = 0$  and  $z_+ = 1$ , moving to the right into the totally unburned region toward  $x \to +\infty$  and leaving behind the totally burned region toward  $x \to -\infty$ .

Example 1.1 A standard example is the reactive Navier–Stokes/Euler system

$$\begin{cases} \partial_t \tau - \partial_x u = 0, \\ \partial_t u + \partial_x p = \partial_x (\nu \tau^{-1} \partial_x u), \\ \partial_t E + \partial_x (pu) = \partial_x (\kappa \tau^{-1} \partial_x T + \nu \tau^{-1} u \partial_x u) + qk \phi(T) z, \\ \partial_t z = \partial_x (d\tau^{-2} \partial_x z) - k \phi(T) z, \end{cases}$$
(2)

where  $\tau>0$  denotes specific volume, u velocity,  $E=e+\frac{1}{2}u^2$  specific gas-dynamical energy, e>0 specific internal energy, and  $0 \le z \le 1$  mass fraction of the reactant, with ideal gas equation of state, single-species reaction, and Arrhenius-type ignition function,

$$p = \frac{\Gamma e}{\tau}, \quad T = c^{-1}e, \quad \phi(T) = e^{\frac{-\varepsilon}{T}}, \tag{3}$$

where  $\Gamma = \gamma - 1 > 0$  is the Gruneisen constant,  $\gamma > 1$  is the adiabatic index, c is specific heat, and  $\mathcal{E}$  is activation energy for the gas [5, 8, 25].

For  $v, \kappa, d > 0$ , this represents the "viscous" (mixed hyperbolic–parabolic) reactive Navier–Stokes (rNS) equations [8, 17], for  $v, \kappa, d = 0$ , the "inviscid" (hyperbolic) reactive Euler, or Zel'dovich–von Neumann–Döring (ZND) equations [18, 83, 84, 87]. These represent successive refinements of the earlier Chapman–Jouget (CJ) theory [14, 38, 39], in which both transport (diffusion) and reaction processes are taken to occur instantaneously, across an ideal shock-like discontinuity.

#### 1.1.1 Inviscid (ZND) Profiles

(Following [90]) In case  $v, \kappa, d=0, r=1$ , we may explicitly solve the profile equation associated with (1), (2), and (3). By the invariances of (2) and (3), we may take without loss of generality  $\tau_+=1, u_+=0, s=1$ , and  $0 \le e_+ \le \frac{1}{\Gamma(\Gamma+1)}$ , with  $\Gamma>0, \mathcal{E}>0, 0 \le q \le q_{CJ}=\frac{(\Gamma+1)^2(\Gamma e_++1)^2-\Gamma(\Gamma+2)(1+2(\Gamma+1)e_+)}{2\Gamma(\Gamma+2)}$ , yielding (substituting  $\partial_t\to\partial_x$  and integrating the conservative  $(\tau,u,E)$  equations)

$$\bar{u} = 1 - \bar{\tau}, \quad \bar{e} = \frac{\bar{\tau}(\Gamma e_+ + 1 - \bar{\tau})}{\Gamma},$$

$$\bar{\tau} = \frac{(\Gamma + 1)(\Gamma e_+ + 1) - \sqrt{2\Gamma(\Gamma + 2)(q_{CJ} - q(\bar{z} - 1))}}{\Gamma + 2}.$$
(4)

The  $\bar{z}$  component can then be solved via  $\bar{z}' = k\phi(c\bar{e}(\bar{z}))z$  on x < 0 (reaction zone). A nonreactive "Neumann shock" at x = 0 connects the ignited state at  $x = 0^-$  to a quiescent state at  $x = 0^+$  (for both of which z = 1), and the profile remains

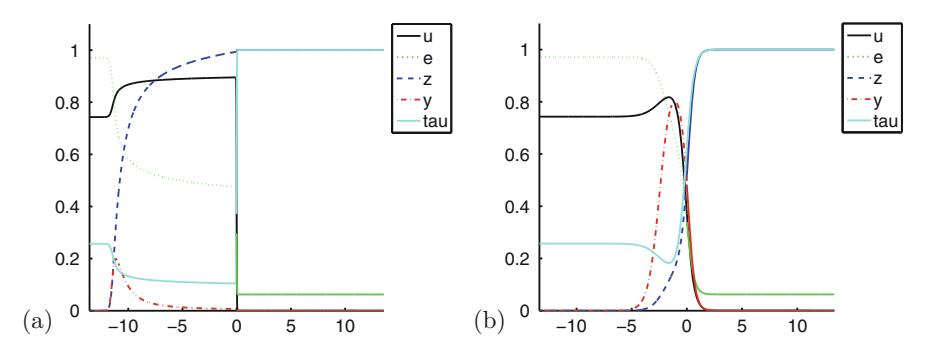


Fig. 1 Sample profiles illustrating diffusive effects. (a)  $v = d = \kappa = 0.01$ . (b)  $v = d = \kappa = 0.3$ . In both cases the reaction zone structure is clearly visible, but in (b) the shock width is of a similar order as the reaction zone width For both plots,  $e_+ = 6.23 \times 10^{-2}$ ,  $k = 1.53 \times 10^4$ ,  $q = 6.23 \times 10^{-1}$ ,  $\mathcal{E} = 6$ ,  $\Gamma = 0.2$ ,  $c_v = 1$ 

constant thereafter, i.e., for all  $x \ge 0^+$ . This corresponds to the physical picture of a gas-dynamical shock moving into an unburned, quiescent gas at  $x \to +\infty$ , which, its temperature being raised by compression of the shock, ignites and burns steadily, leaving a "reaction spike" in its wake, with completely burned gas at  $x \to -\infty$ .

### 1.1.2 Viscous (rNS) Profiles

Likewise, parametrized by  $(e_+, q, \mathcal{E}, \Gamma, \nu, \kappa, d) \in \text{compact domain (i.e., with nonphysical value } e_+ = 0 \text{ adjoined)}$ , rNS profiles are exponentially convergent to their endstates except at the degenerate "Chapman–Jouget" value  $q = q_{CJ}$  [53, 88, 90], for which they decay algebraically. Existence of rNS profiles for small viscosity/heat conduction/species diffusion has been shown, for example, in [28, 86], by singular perturbation of the ZND case. When diffusion coefficients are not small, profiles must be found in general numerically [5]. Numerically determined profiles for different values of diffusion coefficients are displayed in Fig. 1.

### 1.1.3 Issues and Objectives

Unlike nonreactive shocks, which are typically quite stable, detonations frequently exhibit instabilities of different types. See Fig. 2 depicting results of shock tube experiments carried out by John H.S. Lee (reprinted from [50] with permission of the author), which indicates the variety of possible behaviors as physical parameters are varied, from a nonreactive shock-like coherent planar detonation layer, to apparent bifurcation to cellular or pulsating patterns, to what appears to be chaotic flow.

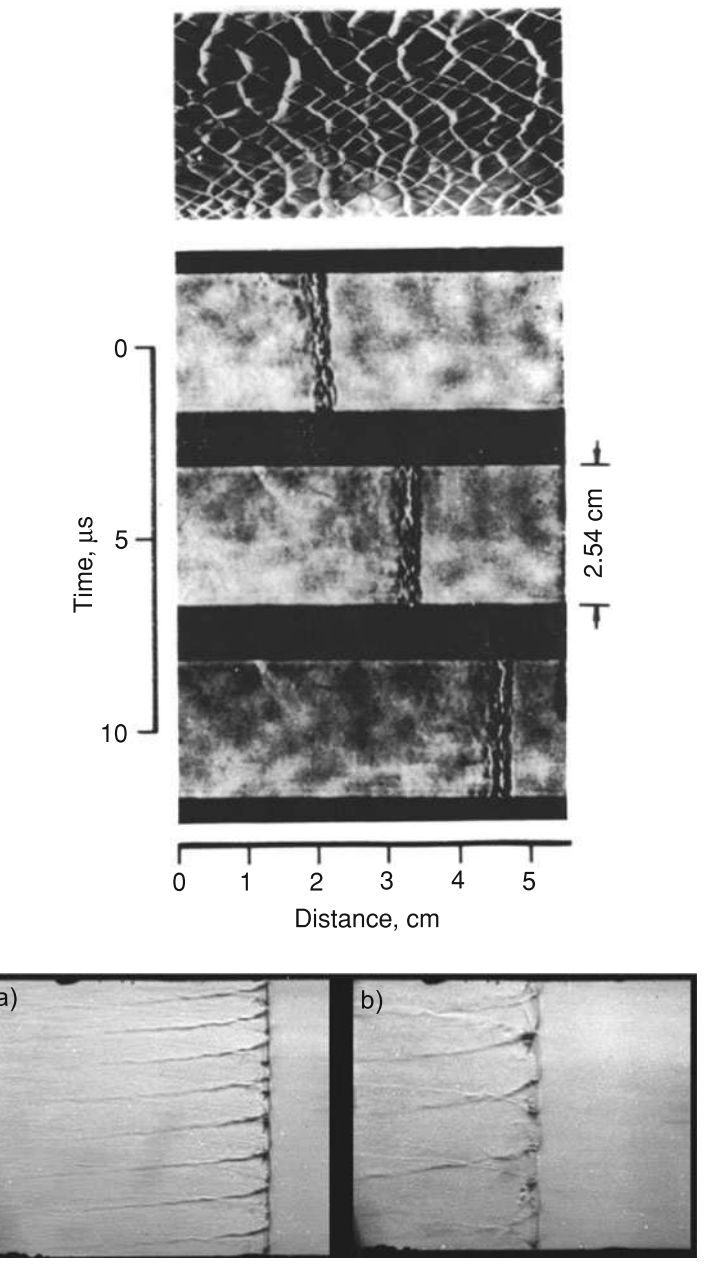


Fig. 2 Detonation instability in a duct (John H.S Lee, McGill University)

The first mathematical model of detonation, the *Chapman–Jouget* model (~1890s; e.g., [14, 38, 39]) treated detonations as a shock modified by instantaneous reaction. This is sufficient to predict possible endstates and speeds of planar discontinuities, but not to determine realizability by a connecting longitudinal reaction/dissipation structure. Moreover, it does not capture the complicated instability/bifurcation phenomena described above; indeed, for the one-step polytropic model of Example 1.1, Chapman-Jouget detonations are *universally stable* [40, 60].

The modern theory of detonation stability dates from the post-world war II period, with the introduction of the ZND mdel [18, 83, 84, 87] and the pioneering stability/behavior studies of J.J. Erpenbeck and others. The ZND model has successfully modeled a wide range of experimentally observed phenomena in stability/behavior. Indeed, there is by now a comparatively long history (~1960s; e.g., [19]), and extensive numerical and analytical literature in the context of ZND; see, for example, [10, 12, 17, 19, 25, 41, 49], and references therein. By contrast, until recently (~1990s; e.g. [53]), there was relatively little investigation of the more complicated rNS model.

**Issues:** 1. Experimental stability transitions/bifurcation to time-periodic pulsating/cellular wave patterns are well modeled by ZND. But, there is no corresponding nonlinear stability or bifurcation theory, and little regularity (or even well-posedness) for the (hyperbolic) equations. 2. The rNS equations on the other hand feature better regularity/well-posedness, but are significantly more complicated; till recently, there was neither linear data nor nonlinear theory. Practical effects/importance of added transport (viscosity/heat conduction/diffusion) terms is not clear.

**Objectives:** 1. Review and rigorous (analytical) verification of physical conclusions plus systematic (numerical/analytical) exploration of parameter space; justification (and improvement) of numerics, for both (ZND) and (rNS). 2. Systematic comparison between and synthesis of (rNS) and (ZND).

## 1.2 Stability Framework: Normal Modes Analysis for ZND

(Following [40]) Shifting to coordinates  $\tilde{x} = x - st$  moving with the background Neumann shock, write the ZND version  $\varepsilon = 0$  of (1) as

$$W_t + F(W)_x = R(W),$$

where

$$W := \begin{pmatrix} u \\ z \end{pmatrix}, \quad F := \begin{pmatrix} f(u) - su \\ -sz \end{pmatrix}, \quad R := \begin{pmatrix} qkz\phi(u) \\ -kz\phi(u) \end{pmatrix}.$$

### 1.2.1 Fixed-Boundary Formulation

Defining the Neumann shock location as X(t), we reduce to a fixed-boundary problem by the change of variables  $x \to x - X(t)$ . In the new coordinates,

$$W_t + (F(W) - X'(t)W)_x = R(W), \quad x \neq 0,$$

with jump condition

$$X'(t)[W] - [F(W)] = 0,$$

 $[h(x,t)] := h(0^+,t) - h(0^-,t)$  denoting the jump at x = 0 of a function h.

### 1.2.2 Linearized Equations

Linearizing about  $(\bar{W}^0, 0)$ , we obtain the *linearized equations* 

$$(W_t - X'(t)(\bar{W}^0)'(x)) + (AW)_x = EW,$$
 (5)

$$X'(t)[\bar{W}^0] - [AW] = 0, \quad x = 0,$$

where  $A = A(x) := (\partial/\partial W)F(\bar{W}^0(x))$ ,  $E = E(x) := (\partial/\partial W)R(\bar{W}^0(x))$ . (Here and below, E is a matrix-valued function, not to be confused with specific energy density in Example 1.1.)

## 1.2.3 Reduction to Homogeneous Form

To eliminate the front from the interior equation, reverse the original transformation to linear order by the change of dependent variables  $W \to W - X(t)(\bar{W}^0)'(x)$ , motivated by  $W(x - X(t), t) - W(x, t) \sim -X(t)W_x(x, t) \sim -X(t)(\bar{W}^0)'(x)$  approximating to linear order the original, nonlinear transformation. (As noted in [40], this can be viewed as a simplified version of the "good unknown" of Alinhac [3, proof of Prop. 3.1].) Substituting using  $(A(\bar{W}^0)(\bar{W}^0)'(x))_x = E(\bar{W}^0)(\bar{W}^0)'(x)$  gives

$$W_t + (AW)_x = EW (6)$$

with modified jump condition  $X'(t)[\bar{W}^0] - [A(W + X(t)(\bar{W}^0)')] = 0$ .

### 1.2.4 Generalized Eigenvalue Equation

Seeking normal mode solutions  $W(x,t) = e^{\lambda t}W(x)$ ,  $X(t) = e^{\lambda t}X$  yields the generalized eigenvalue equations  $(AW)' = (-\lambda I + E)W$ ,  $x \neq 0$ ,  $X(\lambda[\bar{W}^0] - [A(\bar{W}^0)']) - [AW] = 0$ , where "'' denotes d/dx, or, setting Z := AW, to

$$Z' = GZ, \quad x \neq 0, \tag{7}$$

$$X(\lambda[\bar{W}^0] - [A(\bar{W}^0)']) - [Z] = 0, \quad x = 0,$$
 (8)

where  $G := (-\lambda I + E)A^{-1}$ .

## 1.2.5 Stability Determinant

We define the Evans-Lopatinski determinant

$$D_{ZND}(\lambda) := \det \left( Z_1^-(\lambda, 0), \cdots, Z_n^-(\lambda, 0), \lambda[\bar{W}^0] - [A(\bar{W}^0)'] \right)$$
  
= \det \left( Z\_1^-(\lambda, 0), \cdots, Z\_n^-(\lambda, 0), \lambda[\bar{W}^0] + A(\bar{W}^0)'(0^-) \right),

where  $Z_j^-(\lambda, x)$  are a basis of solutions of the interior equations (7) decaying as  $x \to -\infty$ . By  $A(\bar{W}^0)' = dF(\bar{W}^0)(\bar{W}^0)' = R(\bar{W}^0)$  plus duality, we can rewrite this in the simpler form

$$D_{ZND}(\lambda) = \tilde{Z}_n^-(\lambda, 0) \cdot \left(\lambda[\bar{W}^0] + R(\bar{W}^0)(0^-)\right)$$
(9)

useful for numerics [11, 34] and also analysis [90, 91], where  $\tilde{Z}_n^-$  is a (unique up to constant multiple) solution of the dual equation  $\tilde{Z}' = -G^*\tilde{Z}$  decaying as  $x \to -\infty$ . The function  $D_{ZND}$  is exactly the *stability function* derived in a different form by Erpenbeck [6, 19].

• Evidently,  $\lambda$  is a generalized eigenvalue iff  $D_{ZND}(\lambda) = 0$ .

**Definition 1.2** A ZND profile is spectrally stable if there are no zeros of the associated Lopatinski determinant in  $\{\lambda: \Re \lambda \geq 0\} \setminus \{0\}$  [19]. (By translation-invariance, there is always a zero at  $\lambda = 0$ .)

## 1.3 Normal Modes Analysis for rNS

Taking without loss of generality s=0 (i.e., working in co-moving coordinates), write the (rNS) version  $\varepsilon=1$  of (1) as

$$W_t + F(W)_x = (\mathcal{B}(W)W_x)_x + R(W),$$

so that the background detonation wave is an equilibrium  $W(x, t) \equiv \bar{W}^0(x)$ . The linearized eigenvalue equations take the form

$$\lambda W = LW := -(A(x)W)_x + \varepsilon(\mathcal{B}(x)W_x)_x + EW$$

with appropriate A,  $\mathcal{B}$ , E, where  $E = (\partial/\partial W)R(\bar{W}^0(x))$  as in (5). These may be written as a first-order system

$$\mathcal{Z}' = \mathcal{A}(x,\lambda)\mathcal{Z}$$

where  $\mathcal{Z} = \begin{pmatrix} Y \\ W_2 \end{pmatrix} = \begin{pmatrix} AW - \varepsilon \mathcal{B}W_x \\ W_2 \end{pmatrix}$  is an augmented "flux" variable [90].

Define the Evans function

$$D_{rNS}(\lambda) := \det(\mathcal{Z}_{1}^{-}, \dots, \mathcal{Z}_{k}^{-}, \mathcal{Z}_{k+1}^{+}, \dots, \mathcal{W}_{\mathcal{N}})|_{x=0}$$
 (10)

where  $\{\mathcal{Z}_1^-, \dots, \mathcal{Z}_k^-\}(\lambda, x)$  and  $\{\mathcal{Z}_{k+1}^+, \dots, \mathcal{Z}_N\}(\lambda, x)$  are bases of solutions decaying as  $x \to \infty$  and  $x \to +\infty$ .

• Evidently,  $\lambda$  is an eigenvalue iff  $D_{rNS}(\lambda) = 0$ .

**Definition 1.3** An rNS profile is spectrally stable if there are no zeros of the associated Evans function in  $\{\lambda: \Re \lambda \geq 0\} \setminus \{0\}$  [53, 55, 82]. (As for ZND, there is always a zero at  $\lambda = 0$ .)

## 1.4 Abstract Viscous Stability Results

Let  $\{\bar{W}^{\varepsilon}\}\$  be a one-parameter family of viscous strong detonation waves for rNS with polytropic equation of state (3), with associated parameters  $q^{\varepsilon}$ , etc.

### 1.4.1 Spectral Stability Transitions

(Following [53])

**Lemma 1.4 (Stability in the small-heat release limit [53])** *If*  $q^{\varepsilon} \to 0$  *as*  $\varepsilon \to 0$ , *then*  $\{\bar{W}^{\varepsilon}\}$  *is spectrally stable for*  $\varepsilon$  *sufficiently small.* 

**Lemma 1.5** (Absence of steady bifurcations [53]) For all  $\varepsilon$ , the associated Evans function has a zero of multiplicity one at  $\lambda = 0$ :  $D(\varepsilon, 0) = 0$ , and  $D'(\varepsilon, 0) \neq 0$ , hence stability transitions if they occur involve passage of nonzero conjugate zeros across the imaginary axis. More generally, this holds for any equation of state for which the associated CJ profiles are stable

Lemma 1.4 is an immediate consequence of the construction of an Evans function, done similarly as in [2, 27], using the resulting continuity with respect to parameters together with decoupling at q=0 of gas-dynamical (u) and reaction (z) equations. Lemma 1.5 follows by a "stability index" computation like those of [27, 66, 93], quantifying the intuition that low-frequency behavior of rNS should "not see" reaction and transport scales, so should reduce to that of CJ. See [40] for a far-reaching extension of this principle including also ZND and multi-D.

*Takeaways:* 1. Stable waves exist. 2. Stability transitions should they occur are of (spectral) Hopf, i.e., "pulsating" type, *as seen in experiment-* and, indeed, they are seen numerically to occur, as displayed, for instance, in Fig. 7 below. (Link between behavior and equations.)

## 1.4.2 Nonlinear Stability/Difurcation Criteria

(Following [82])

**Theorem 1.6 (Spectral**  $\Rightarrow$  **nonlinear stability [82])** For all  $\varepsilon$ ,  $\bar{W}^{\varepsilon}$  is  $L^1 \cap L^p \to L^p$  linearly orbitally stable if and only if the only zero of  $D(\varepsilon, \cdot)$  in  $\Re \lambda \geq 0$  is a simple zero at the origin, in which case  $\bar{W}^{\varepsilon}$  is  $L^1 \cap H^3 \to L^1 \cap H^3$  linearly and nonlinearly orbitally stable, with

$$|\tilde{W}^{\varepsilon}(\cdot,t) - \bar{W}^{\varepsilon}(\cdot - \delta(t))|_{L^{p}} \leq C|\tilde{W}_{0}^{\varepsilon} - \bar{W}^{\varepsilon}|_{L^{1} \cap H^{3}}(1+t)^{-\frac{1}{2}(1-\frac{1}{p})},$$

for nearby solutions  $\tilde{W}^{\varepsilon}$ , where

$$|\delta(t)| \leq C|\tilde{W}_0^{\varepsilon} - \bar{W}^{\varepsilon}|_{L^1 \cap H^3}, \quad |\dot{\delta}(t)| \leq C|\tilde{W}_0^{\varepsilon} - \bar{W}^{\varepsilon}|_{L^1 \cap H^3}(1+t)^{-\frac{1}{2}}.$$

**Theorem 1.7 (Spectral**  $\Rightarrow$  **nonlinear bifurcation [82])** Assume that  $\bar{W}^{\epsilon}$  undergoes transition from linear stability to linear instability at  $\epsilon = 0$ , via passage of a single complex conjugate pair of eigenvalues  $\lambda_{\pm}(\epsilon) = \gamma(\epsilon) + i\tau(\epsilon)$  through the imaginary axis:

$$\gamma(0) = 0, \quad \tau(0) \neq 0, \quad d\gamma/d\varepsilon(0) \neq 0.$$
 (11)

Then, given exponential weight  $\omega > 0$ , for  $0 \le r \ll 1$ ,  $C \gg 1$ , there are  $C^1$  functions  $r \to \varepsilon(r)$ , T(r), with  $\varepsilon(0) = 0$ ,  $T(0) = 2\pi/\tau(0)$ , and a  $C^1$  family of time-periodic solutions  $\tilde{U}^r(x,t) \in H^2_\omega$  of (rNS) with  $\varepsilon = \varepsilon(r)$ , of period T(r), with  $C^{-1}r \le r$ 

 $\|\tilde{U}^r - \bar{U}^\varepsilon\|_{H^2_\omega} \le Cr$ , where  $\|f\|_{H^2_\omega} := \|\omega f\|_{H^2}$  and  $H^2_\omega$  is the space determined by  $\|\cdot\|_{H^2_\omega}$ . Up to translation in x, t, these are locally unique in  $\|\cdot\|_{H^2_\omega}$ .

Theorem 1.6 is established by detailed pointwise Green bounds obtained from stationary phase type estimates on the inverse Laplace transform representation of the linearized solution operator, together with a nonlinear shock tracking argument, in the spirit of [61, 89, 92]. Theorem 1.7 is established by a novel "reverse temporal dynamics" argument using inverse Laplace transform estimates similar to those for stability. See also [73, 80, 81] for related studies in the shock wave case. For a nonlinear stability analysis of the bifurcating time-periodic solutions, see [9]. *Takeaways:* 1. Rigorous characterization (with Lemma 1.5) of 1d instability as Hopf bifurcation. 2. Spectral information as in Lemmas 1.4 and 1.5 translates to full nonlinear results.

### 1.4.3 Closing the Philosophical Loop: The rNS→ZND Limit

(Following [90]) At this point, the situation as regards the two theories (rNS and ZND) is that we have for ZND decades of spectral stability data, numerics, and formal asymptotics, but no nonlinear theory; for rNS, we have essentially the reverse. A way to repair this situation, combining the strengths of the two theories, is to link them via the vanishing viscosity, rNS $\rightarrow$ ZND limit. The limiting profile structure problem has been studied in [28, 86], etc., with definitive results. However, until recently, the only analytical result regarding stability was the study by Roquejoffre–Vila [72] for *Majda's model* [58], a simplified qualitative model of detonations. A generalization to the full rNS system is as follows; here,  $\bar{W}^{\varepsilon}$  represents an  $\varepsilon$ -profile, with  $\varepsilon$  measuring size of transport (viscosity/heat conduction/diffusion) coefficients.

**Theorem 1.8 (rNS spectrum in the ZND limit [90])** Spectral stability of  $\bar{W}^{\varepsilon}$  for  $\varepsilon > 0$  sufficiently small is equivalent to spectral stability of the limiting ZND detonation  $\bar{W}^0$  together with spectral stability of the viscous version of the associated Neumann shock. Moreover, (i) For  $C \le |\lambda| \le C/\varepsilon$ , C sufficiently large, on  $\Re \lambda > -\eta$  for  $\eta$ ,  $\varepsilon > 0$  sufficiently small,  $\varepsilon$  times the set of zeros of  $D_{rNS}^{\varepsilon}$  converges to the set of zeros of  $D_{rNS}^{\varepsilon}$  on  $\Re \lambda \ge 0$ . (ii) For  $|\lambda| \le C_0$ ,  $C_0$  arbitrary, on  $\Re \lambda \ge -\eta < 0$ , the zeros of  $D_{rNS}^{\varepsilon}$  converge in location/multiplicity as  $\varepsilon \to 0$  to the zeros of  $D_{ZND}$ .

The proof of Theorem 1.8 is by detailed multi-scale analysis as in stability of strong shocks and other asymptotic limits [36, 68], together with an  $\varepsilon$ -variational argument like that used in [27] and [93] to study the related low-frequency (small- $\lambda$ ) limit. The detailed asymptotics provided on the profile by the analyses of [28, 86] are used in an important way. It is known that nonreactive viscous shocks of a polytropic gas are universally stable [33, 35], hence the theorem *reduces spectral stability for rNS in the small-viscosity limit to spectral stability of ZND*.

*Takeaways:* 1. Verifies NS stability/bifurcation for small  $\varepsilon$  through extensive existing numerical studies for ZND. 2. Gives rigorous nonlinear sense to (spectral) ZND results.

This gives one answer to the question "what is the role of viscosity?" (namely, an element in logical development/foundations, with little effect on phenomena). We'll explore a possible different answer below, in Sect. 1.7.

## 1.5 Abstract Inviscid Stability Results

(First rigorous stability results for ZND) Let  $\{\bar{W}^{\varepsilon}\}$  be a one-parameter family of strong detonation waves for ZND with polytropic equation of state (3).

To explain our next results, we first recall that the parametrization given in Sect. 1.1.1 is not the standard one given in the literature, but our own improved version [90]. In the classical parametrization given e.g. in [21],  $e_+$  rather than speed s is held fixed, and the detonation parametrized rather by the *overdrive*  $1 < f < \infty$ , defined as the square of the ratio of relative speed of the detonation (with respect to the ambient gas) and the minimum, Chapman–Jouget, detonation speed among all possible strong detonations [10, 21, 26, 49]. In this classical scaling, two rules of thumb observed numerically are that detonations are more stable the smaller the heat release q and the higher the overdrive f. The former was proved by Erpenbeck for finite frequencies, but his treatment of high frequencies was incomplete [91].

**Lemma 1.9 (Stability in the small-heat release limit [91])** In the scaling of Sect. 1.1.1, if  $q^{\varepsilon} \to 0$  as  $\varepsilon \to 0$ , then  $\{\bar{W}^{\varepsilon}\}$  is spectrally stable for  $\varepsilon$  sufficiently small.

**Corollary 1.10 (Stability in the high-overdrive limit [91])** *In the scaling of Erpenbeck [21], ZND detonations of (3) are spectrally stable in the fixed-activation energy, fixed-heat release, high-overdrive limit*  $f \to \infty$ .

The first result includes but is not restricted to the observation of Erpenbeck that, in the scaling of [21], ZND detonations are stable in the fixed-activation energy, fixed-overdrive, small-heat release limit, which in our scaling corresponds to fixed-activation energy, fixed- $e_+$  or shock strength, and small-q or heat release. The second result, corresponding in our scaling to stability in the simultaneous *zero-heat release*, *zero-activation energy*  $\mathcal{E}$ , and *strong-shock* (zero- $e_+$ ) *limits*, resolves an open problem from [21]. Our favorable coordinatization (s=1 held fixed,  $e_+ \to 0$ ), suggested by similar scalings used to study the strong-shock limit for gas dynamics [35, 36], plays an important role in the analysis. For, this keeps all quantities bounded for bounded frequencies, independent of parameters, allowing uniform treatment of the strong-shock limit. By contrast, internal energy e and temperature T blow up for the classical scaling in the strong-shock limit. In the course of the proof, specifically in treating the complementary regime of frequencies

going to infinity, we establish also 1D high-frequency stability, along with new asymptotic ODE techniques.

*Takeaways:* 1. Analytical signposts guiding delicate/computationally intensive numerics [19, 49]. 2. 1D high-frequency stability, validating the necessary truncation of computational (i.e., frequency) domain in carrying out numerical stability studies. (See Sect. 2 for further discussion.)

Remark 1.11 The 1-D high-frequency stability analysis foreshadows issues addressed in Sect. 2.1 for multi-D. Notably, the 1D analysis requires only  $C^2$  regularity on coefficients/equation of state.

## 1.6 Numerical Results for ZND

#### 1.6.1 Natural Coordinatization

The novel scaling introduced in Sect. 1.1.1 is helpful not only for rigorous analysis, as seen in Sect. 1.5, but also at the level of numerics/modeling. In Fig. 3, we display in the classical scaling of Erpenbeck [21] results for a standard benchmark problem of Fickett and Woods [21, 26, 49], holding overdrive f fixed and varying activation energy  $\mathcal{E}_0$  and heat release  $Q_0$ , with  $\Gamma=1.2$ . The solid curves depicted are the *neutral stability curves* across which detonations change from stable (below) to unstable (above) as  $\mathcal{E}_0$  is increased. In this figure, we see the stabilizing effect

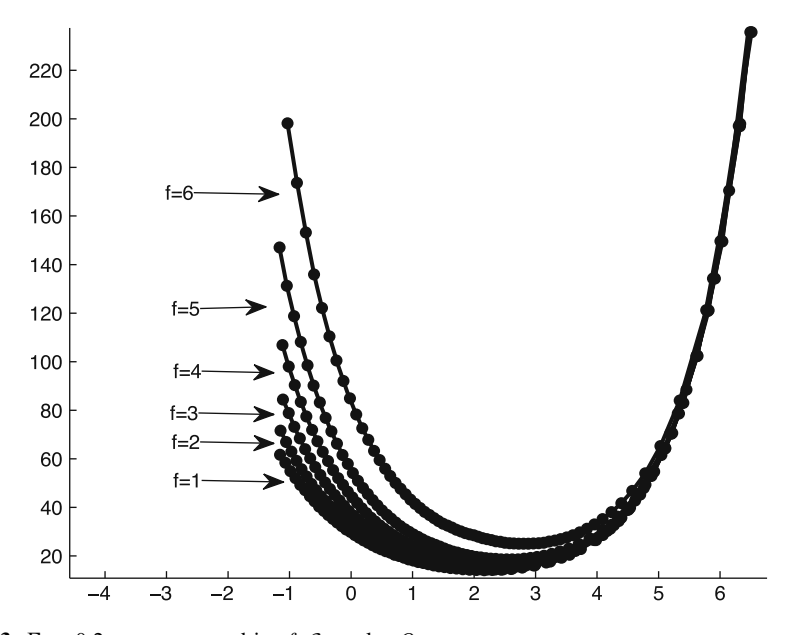


**Fig. 3**  $\Gamma = 0.2$ , constant overdrive f,  $\mathcal{E}_0$  vs.  $\log Q_0$ 

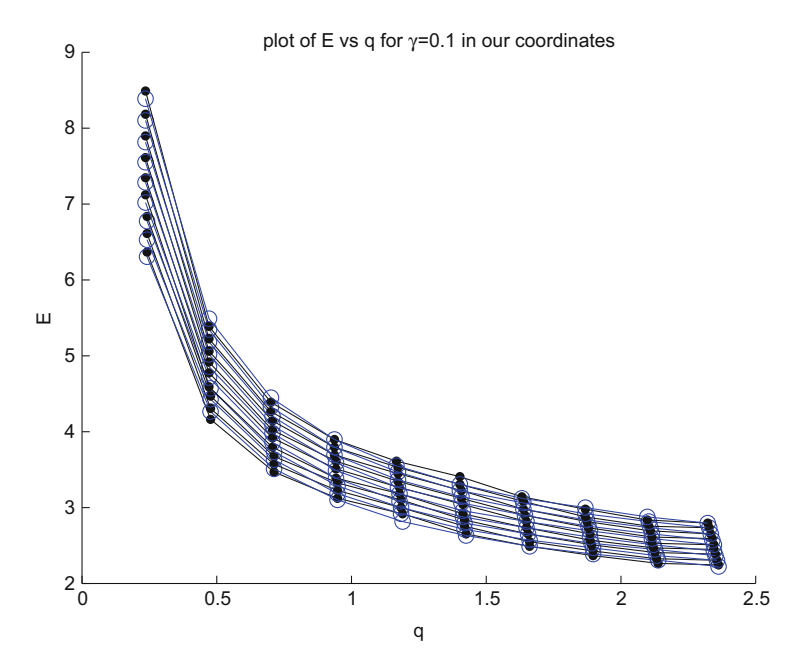


**Fig. 4**  $\mathcal{E} = \mathcal{E}_0 e_+$  vs.  $q = Q_0 e_+$ ; polynomial fit, average relative error 1%

of increasing f and the destabilizing effect of increasing  $\mathcal{E}_0$ ; however, there is an apparent hysteresis effect as  $Q_0$  is increased, with detonations first destabilizing, then restabilizing for large  $Q_0$ . Moreover, there is a singularity at the right of the diagram with  $\mathcal{E}_0, Q_0 \to \infty$ .

In Fig. 4, we depict the analogous neutral stability curves for the same gas constant  $\Gamma=1.2$  in *our* scaling (the one of Sect. 1.1.1), with  $e_+$  held fixed and  $\mathcal{E}=\mathcal{E}_0e_+$  and  $q=Q_0e_+$  varying. In these coordinates, both hysteresis and singularity are removed. The latter allows us to verify numerically *stability in the zero-activation energy limit*:  $\mathcal{E}=0 \Rightarrow \text{ZND}$  stability for any  $q, e_+$ .

Moreover, the neutral stability curves follow a simple and regular pattern, as may be seen most dramatically in the log-log plot of Fig. 5. Indeed, a naive polynomial fit with 20 stored coefficients is sufficient to recover the entire diagram in seconds with 2% minimum/1% average accuracy, a considerable compression of data for a diagram that requires hours to compute (see data below).

### 1.6.2 Computational Improvements

Besides the improvement in parametrization described above, we have by adapting to detonation theory numerical Evans function algorithms developed for the study of viscous shock stability [4], improved computation speed by a factor of 1–2 orders of magnitude compared to the current state of the art as described, e.g., in [49, 78];

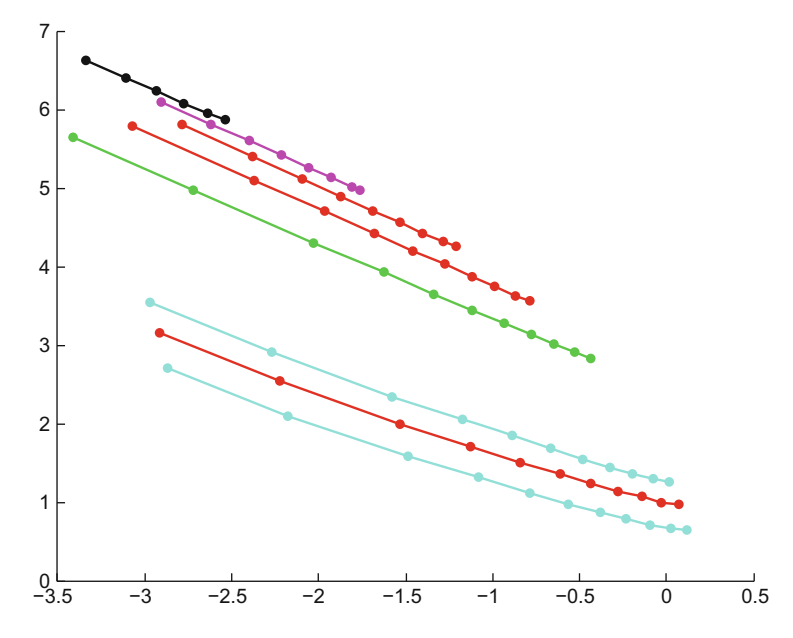


**Fig. 5**  $\log \mathcal{E}$  vs.  $\log q$ 

see [6, 37]. With these improvements, combined with vastly improved hardware capability, what took 5 h on a supercomputer in 1990 to compute a single fixed-overdrive curve today takes 5 h on a Mac Quad Duo to compute the full Fig. 3. Indeed, this can be carried out perfectly well on a laptop.

We are now able to not only compute neutral stability curves, but to accurately describe all unstable eigenvalues even for large activation energies; see for example the eigenvalue configuration displayed in Fig. 7(left) for the same benchmark problem studied in Figs. 3 and 4 at activation energy  $\approx$ 7.1, for which we accurately resolve a pattern of  $\approx$  50 unstable roots using code supported in the MATLAB-based openware package STABLAB [4].

## 1.7 Numerical Results for rNS

Improvements in computations/power have made possible for the first time numerical Evans investigations for rNS, a substantially more intensive problem than ZND. These investigations, though just beginning, have already yielded surprising results.

## 1.7.1 "Viscous Hyperstabilization"/Hysteresis

(Following [5]) For the benchmark problem discussed in Sect. 1.6, Romick et al [70, 71] have carried out numerical time-evolution studies indicating a significant delay in transition to instability as activation energy is increased for the viscous (rNS) problem as compared to the inviscid (ZND) one: as much as 10% for values of viscosity in the high range of physically relevant scales. Our numerical Evans investigations both confirm and extend these observations, indicating not only the expected delay but also a new type of hysteresis in which viscous detonations eventually restabilize as activation energy is increased still further [5]. This striking phenomenon is depicted in Fig. 6(left); see Fig. 6(right) for a graph of viscous delay vs. viscosity. We call this phenomenon viscous hyperstabilization; we have conjectured [5] that it occurs for any nonzero viscosity, no matter how small.

Note the slow, apparently logarithmic, growth, in the upper stability boundary of Fig. 6(left) as viscosity goes to zero, suggesting that hyperstablization might play a relevant physical role even for quite small values of viscosity. Another notable feature of Fig. 6(left) is the "nose" to the right of the neutral stability curve, where upper and lower boundaries meet. This indicates that there is *no instability*, regardless of the value of  $\mathcal{E}$ , for sufficiently large viscosity. For reference, the viscosity values considered in [70, 71] correspond to  $\nu = 0.1$  in the scaling of Fig. 6; see [5, §3.5]. As discussed in [5, 70, 71], this appears to be roughly an order of magnitude higher than in typical physical situations. A more realistic value would be  $\nu = .01$ .

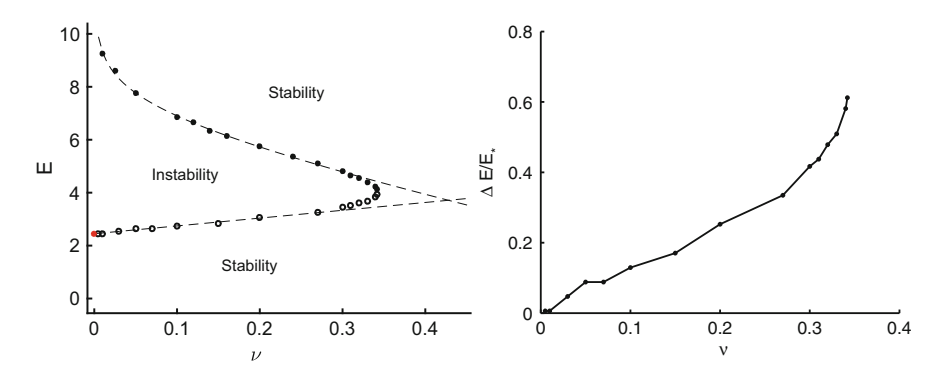


**Fig. 6** Left: Neutral Stability Boundaries in the  $\mathcal{E}$ - $\nu$  plane. The best-fit curve (dashed line,  $\nu < 0.27$ ) for the upper boundary is  $\mathcal{E}^+(\nu) = 5.67 - 6.16\nu - 0.804 \ln(\nu)$ . The red dot denotes the ZND (inviscid) stability boundary (lower boundary only!). Right: Viscous delay (cf. [70, 71]): We plot  $\Delta E/\mathcal{E}_* = (\mathcal{E}^-(\nu) - \mathcal{E}_*)/\mathcal{E}_*$  against  $\nu$ , where  $\mathcal{E}_*$  is the approximation to the ZND neutral boundary. Here,  $\nu = d = \kappa$ ,  $\Gamma = 0.2$ ,  $e_+ = 6.23 \times 10^{-2}$ , and  $q = 6.23 \times 10^{-1}$  are held fixed

## 1.7.2 Associated Eigenvalue Distributions

The restabilization phenomenon just described is the more remarkable given the details of the unstable eigenvalue distribution. In the inviscid case, it is more or less a universal principle that increasing  $\mathcal E$  increases instability [21, 25, 49]; indeed, as  $\mathcal E$  increases, more and more unstable eigenvalues cross the imaginary axis from stable to unstable complex half-plane never to return, in a cascade of Hopf bifurcations.

In Fig. 7(left) we display the eigenvalue distribution at  $\mathcal{E} \approx 7.1$ , for which there are 48 unstable roots together with the translational eigenvalue at  $\lambda=0$ ; further increases in  $\mathcal{E}$  lead to further unstable eigenvalues. In Fig. 7(right) we display for contrast the behavior of rNS eigenvalues for the value of viscosity  $\nu=0.1$  considered in [70, 71], tracking the unstable eigenvalues as  $\mathcal{E}$  is varied through the stability transition region. For this viscous case, we find that there are *just two* pairs of unstable eigenvalues in total, which after crossing the imaginary axis to the right turn back and rather quickly restabilize by crossing back into the stable half-plane; meanwhile, the nearby inviscid eigenvalues plotted in the same figure may be seen to continue to the right. At the value  $\mathcal{E} \approx 7.1$  corresponding to the display of unstable inviscid eigenvalues in Fig. 7(left), there are *no remaining* unstable eigenvalues for the viscous case with  $\nu=0.1$ .

*Takeaways:* 1. Another possible answer to the question "what is the role of viscosity" in stability of strong detonations (namely, as a mediator in physical phenomena, and not only an element in mathematical theory). 2. A potentially important physical effect, meriting further study.

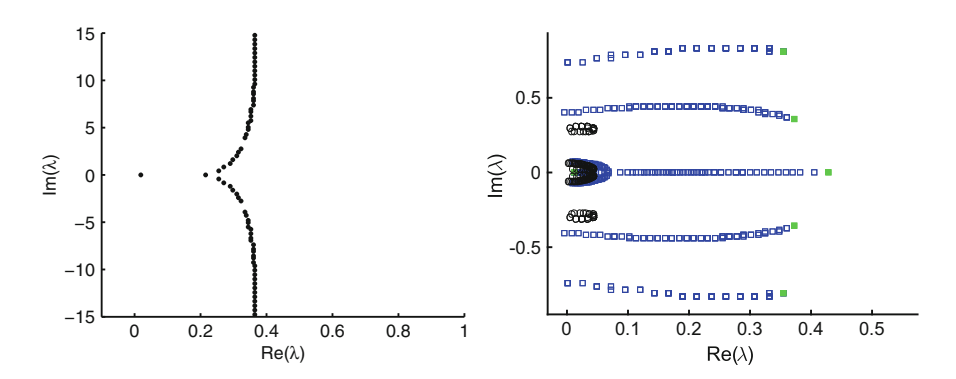


Fig. 7 Left: 48 unstable eigenvalues for ZND,  $\mathcal{E}=7.1$ ; none for rNS! Right: The movement of unstable roots in the complex plane as  $\mathcal{E}$  increases. Circles mark rNS roots, open squares ZND roots. The smaller modulus rNS roots enter for  $\mathcal{E}\approx2.75$  and the larger modulus roots for  $\mathcal{E}\approx3.65$ . The large modulus roots have a turning point at about  $\mathcal{E}\approx5.2$ , and the small modulus roots at  $\mathcal{E}\approx5.5$ . The large modulus roots leave at  $\mathcal{E}\approx6.85$  and the small modulus roots at  $\mathcal{E}\approx6.85$ 

## 1.8 Discussion and Open Problems

Investigation of detonation stability has proceeded by a blend of rigorous analysis, formal asymptotics, and intensive numerical computation; however, the delicacy of these analyses/computations has made definite conclusions elusive. One of the few definitive rules of thumb is that increasing activation energy destabilizes detonations, while increasing overdrive or decreasing heat release stabilizes them. However, this has been difficult to confirm globally due to difficulty/expense of computing for sufficiently large activation energies. We hope that the selection of 1D results we have described indicates a clear role for the type of dynamical systems/Evans function techniques used to study viscous shock wave, both in confirming known rules of thumb/computational results and suggesting new possible directions of investigation—at the same time suggesting roles for viscous theory in providing both rigor and new phenomena.

At the inviscid level, an unexpected bonus has been the discovery of the useful coordinatization of Sect. 1.2, which appears to offer useful guidance/organization of information at the level of applications. It is to be hoped that further analysis (see open problem 3 just below) will identify similar "master coordinates" in the context of rNS, removing the hysteresis of Fig. 6.

Open problems:

- Effects of viscosity on detonation behavior.
- 1D instability of ZND detonations in the high-activation energy limit.
- Viscous stabilization of rNS detonations in the high-activation energy limit.
- Stability of rNS detonations with multistep reactions.
- Stability of weak detonations/deflagrations for rNS (discussed further below).

Regarding the first problem, see the interesting recent discussion by Powers and Paolucci [69] on complicated-chemistry reactions, pointing out that viscous length scales neglected in ZND may be on the same order as reaction scales important for stability. Regarding the second, it has been addressed formally in suggestive fashion by Buckmaster–Neeves, Short, Clavin–He, etc. [13, 15, 75], but up to now (a) not rigorously verified, and (b) as pointed out by Erpenbeck, Lee–Stewart, Short, etc. [19, 49, 75, 76], exhibiting puzzling differences with observed numerics. Both this and the third, hyperstabilization, problem appear to reduce to semiclassical limit/turning-point problems similar to those treated in Sect. 2, with governing parameter  $1/\mathcal{E} \rightarrow 0$ . See also the related [24] for reduced models accurately capturing behavior.

The fourth and fifth problems concern topics omitted in these notes, but in principle treatable by similar techniques. The addition of more physically realistic reaction chemistry complicates but does not essentially change the mathematics; however, as noted by Lee–Stewart and others [49] for ZND, it can significantly affect physical behavior/phenomena. Stability of weak detonation and deflagration waves (alternative types of combustion waves not discussed here [17, 28]) has been studied for simplified "Majda"-type models in [32, 52, 54, 58, 79] and for artificial

viscosity systems in [55]; for a discussion in the context of the full rNS equations, see [82].

## 2 High-Frequency Stability of ZND Detonations and $C^{\infty}$ vs. $C^{\omega}$ Stationary Phase

In this second part, we focus now on a specific topic in multidimensional stability analysis for ZND. A delicate aspect of numerical stability investigations for ZND (inviscid) detonations is truncation of the computational domain by high-frequency asymptotics, a semiclassical limit problem for ODE. In this part, we focus on this issue in the most delicate *multi-D case*, revisiting and completing/somewhat extending the important investigations of this topic by Erpenbeck [22, 23] in the 1960s. This leads to interesting questions related to WKB expansion, turning points, and block-diagonalization/separation of modes. In particular, as we shall describe, it highlights the difference between spectral gap and "spectral separation," revealing essential differences between  $C^{\infty}$ -coefficient and analytic-coefficient theory. These differences are in turn related to oscillatory integrals and differences in stationary phase estimates for  $C^{\infty}$  vs. analytic symbols.

Ouestions we have in mind in this section are:

- Can we complete/make rigorous the turning-point investigations of Erpenbeck?
- What is the meaning, finally, of such *inviscid* high-frequency results?

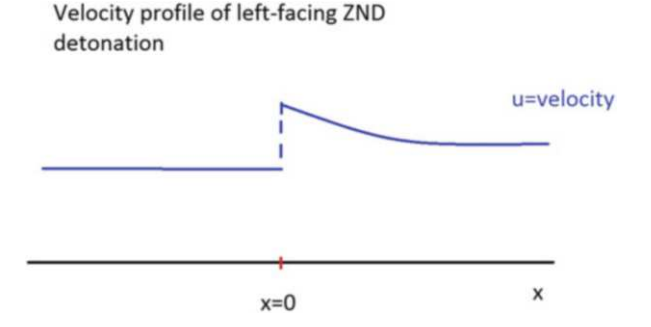
## 2.1 Multi-d Stability of ZND Detonations

The multi-D reactive Euler, or Zel'dovich-von Neumann-Döring (ZND) equations, in Eulerian coordinates, are

$$\begin{cases} \partial_{t}\rho + \nabla_{x} \cdot (\rho u) = 0, \\ \partial_{t}u + \nabla_{x} \cdot (\rho u \otimes u) + \nabla_{x}p = 0, \\ \partial_{t}E + \nabla_{x} \cdot (\rho uE + up) = qk\phi(T)z, \\ \partial_{t}z + \nabla_{x} \cdot (\rho uz) = -k\phi(T)z, \end{cases}$$
(12)

where  $\rho > 0$  is density, u velocity,  $E = e + \frac{1}{2}|u|^2$  specific gas-dynamical energy, e > 0 specific internal energy, and  $0 \le z \le 1$  mass fraction of the reactant, typically with polytropic equation of state and Arrhenius-type ignition function,

$$p = \frac{\Gamma e}{\tau}, \quad T = c^{-1}e, \quad \phi(T) = e^{\frac{-\varepsilon}{T}}. \tag{13}$$



#### 2.1.1 Planar ZND Detonation Waves

A (without loss of generality) standing, "left-facing," planar detonation front is a solution

$$(\rho, u, E, z)(x, t) = \begin{cases} (\rho_{-}, u_{-}, E_{-}, 1), & x_1 < 0, \\ (\bar{\rho}, \bar{u}, \bar{E}, \bar{z})(x_1), & x_1 \ge 0, \end{cases}$$

of (12) with  $(\bar{\rho}, \bar{u}, \bar{E}, \bar{z})(x_1) \to (\rho_+, u_+, E_+, 0)$  as  $x_1 \to +\infty$ . This consists of a nonreactive "Neumann" shock at  $x_1 = 0$ ,  $z(0^{\pm}) = 1$ , pressurizing reactant-laden gas moving from left to right and igniting the reaction. As depicted in Fig. 2.1.1, the profile is constant on  $x_1 \le 0$  and has a reaction tail on  $x_1 \ge 0$ , with burned state z = 0 at  $x_1 = +\infty$ .

### 2.1.2 Spectral Stability Analysis

Consider the abstract formulation of the equations

$$W_t + \sum_{i} \partial_{x_j} F_j(W) = R(W). \tag{14}$$

Similarly as in the 1D case, Sect. 1.2.4, a normal modes analysis leads to the linearized eigenvalue problem [21, 40, 59]  $\lambda A_1^{-1}Z + Z' \sum_{j \neq 1} i \xi_j A_j A_1^{-1}Z = E A_1^{-1}Z'$ , denoting  $\partial_x$ , where  $Z := A_1 W$ ,  $A_j = A_j(x) := (d/dW) F^j(\bar{W}(x))$ , and  $E = E(x) := (d/dW) R(\bar{W}(x))$ ,  $\bar{W}$  the background wave:, or interior equation (written without loss of generality for simplicity in dimension d = 2):

$$Z' = GZ := -(\lambda + \xi A_2 + E)A_1^{-1}Z, \qquad x \ge 0^+,$$

plus a (modified Rankine-Hugoniot) jump condition at x = 0. Here and in what follows, we drop the subscript for x in the eigenvalue ODE, writing  $x_1$  as simply x.

## 2.1.3 Evans-Lopatinski Condition (Erpenbeck's Stability Function)

Normal modes  $e^{\lambda t}e^{i\xi x_2}W(x_1)$ ,  $\Re \lambda \ge 0$  correspond to zeros of the Evans–Lopatinski determinant

$$D_{ZND}(\xi,\lambda) = \tilde{Z}_{1}^{-}(\lambda,0) \cdot (\lambda[\bar{W}] + i\xi[F_{2}(\bar{W})] + R(\bar{W})(0^{+})), \tag{15}$$

where  $[\cdot]$  denotes jump across x = 0 and  $\tilde{Z}_1$  is a (unique up to constant multiplier) solution of the dual equations

$$\tilde{Z}' = -G^* \tilde{Z} = (A_1^*)^{-1} (\lambda + \xi A_2 + E)^* \tilde{Z}$$
(16)

decaying as  $x \to +\infty$ . (This neat formulation, again, due to Jenssen-Lyng-Williams [40].)

Note that (15) reduces for  $\xi = 0$  to the 1D Lopatinski formula (9), the only difference being that we have chosen in this section to analyze *left-going* detonations and in Sect. 2 to analyze *right-doing* detonations, to match the respective source documents [90] and [40]. This has the effect of reversing the order of characteristic modes, so that  $\tilde{Z}_n$  in (9) becomes  $\tilde{Z}_1$  in (15).

## 2.1.4 Comparison to Shock Wave Case

For later, we note that the Evans-Lopatinski determinant described in (15) and (16) is quite similar to that described for the shock wave case in [89, 93], with the differences that here G is variable-coefficient rather than constant-coefficient and  $E, R \not\equiv 0$ . In practice, (15) is computed numerically by approximation of (16) [6, 7, 19, 21, 37].

## 2.2 High-Frequency Stability and the Semiclassical Limit

(Following [44, 45]) We now come to our main topic. The numerics typically used to evaluate (15) are sensitive and computationally intensive, particularly at high frequencies [6, 7, 21, 49]; thus, an important step in obtaining reliable results is to truncate the frequency domain by a separate, high-frequency analysis. Even the few analytically deducible results (stability in  $q \to 0$  or high overdrive limit) require high-frequency truncation as a crucial (and somewhat delicate) step; see Sect. 1. Our purpose here is to: 1. Describe two recent results of Lafitte-Williams-Zumbrun on high-frequency stability [44, 45]: one instability and one stability theorem, building on the pioneering ideas of Erpenbeck's 1960s Los Alamos Technical Report [22, 23]. 2. Discuss related block-diagonalization of semiclassical ODE [46].

### 2.2.1 Formulation as Semiclassical Limit

Setting  $(\xi, \lambda) = h^{-1}(1, \zeta)$ , for  $|\xi| >> 1$ , interior equation (16) becomes the semiclassical limit problem

$$h\tilde{Z}' = (G_0 + hG_1)\tilde{Z},\tag{17}$$

where  $G_0 = -[(\zeta + iA_2)A_1^{-1}]^*$  involves only nonreactive gas-dynamical quantities, so is identical to the symbol appearing in (nonreacting) shock stability analysis,  $G_1$  uniformly bounded,  $h = |\xi|^{-1} \to 0$ . Likewise, the boundary vector  $(\lambda[\bar{W}] + i\xi[F_2(\bar{W})] + R(\bar{W})(0^+))$  appearing in (15) rewrites as

$$h^{-1}(\ell_0 + h\ell_1), \tag{18}$$

where  $\ell_0 = \zeta[\bar{W}] + i[F_2(\bar{W})]$  is as in the nonreactive gas-dynamical case, and  $R(\bar{W}^0)(0^+)$  is bounded. The difference in principal parts from the nonreactive case is just that  $G_0$  is now varying in x.

### 2.2.2 Symbolic Analysis

From the study of nonreactive gas dynamics [20, 59, 74, 89], we know that the eigenvalues of the principal symbol  $G_0$  are

$$\mu_1 = -\kappa(\kappa \zeta + s)/\eta u_1, \quad \mu_2 = -\kappa(\kappa \zeta - s)/\eta u_1, \quad \mu_3 = \mu_4 = \mu_5 = \xi/u_1,$$
 (19)

where  $\kappa = u_1/c_0$ ,  $\eta = 1 - u_1^2/c_0^2$ ,  $c_0 =$ sound speed,

$$s = \sqrt{\zeta^2 + c_0^2 - u_1^2},\tag{20}$$

and, from the profile existence theory (specifically, the *Lax characteristic condition* [47, 48, 77] on the component Neumann shock),

$$c_0^2 - u_1^2 > 0;$$
 (21)

here,  $\mu_1$  and  $\mu_2$  are *acoustic*, and  $\mu_3$ ,  $\mu_4$ ,  $\mu_5$  *entropic* and *vorticity* modes.

Thus, on the domain  $\Re \zeta \geq 0$  relevant to the eigenvalue/stability problem, there is a single decaying mode  $\mu_1$  for  $\Re \zeta > 0$ , which extends continuously to the boundary  $\zeta = i\tau$ . For reference, we will call this the "decaying" mode even at points on the imaginary boundary where it becomes purely oscillatory (as does happen for values of  $\zeta = i\tau$  such that  $\tau^2 \geq c_0^2 - u_1^2$ ). Evidently, the decaying mode  $\mu_1$  remains separated from all other modes  $\mu_j$  except at glancing points for which  $\mu_1 = \mu_2$ , or s = 0: equivalently,  $\zeta = \pm i \sqrt{c_0^2 - u_1^2}$ , a property depending on both x and  $\zeta$ .

Glancing points play a central role in the study of multi-D nonlinear stability of (nonreactive) viscous and inviscid shock and boundary layers [29, 30, 43, 57, 59, 62–64, 88], presenting the chief technical difficulty in obtaining sharp linear resolvent bounds needed to close a nonlinear analysis. There, the issue is to obtain bounds on a constant-coefficient symbol as frequencies  $\xi$ ,  $\lambda$  are varied in the neighborhood of a glancing point. In the present context, the problem is essentially dual: *for fixed frequencies*  $\zeta$  *to understand the flow of ODE* (17) *as the spatial coordinate x is varied*, a nice twist for experts in shock theory. This leads us naturally to WKB expansion/turning point theory, where glancing points represent *nontrivial turning points*.

## 2.2.3 Analysis of (17) by WKB Expansion/Approximate Block-Diagonalization

The situation of ODE (17), where solutions vary on a much faster scale  $\sim h^{-1}$  vs.  $\sim 1$  than coefficients, is precisely suited for approximation by WKB expansion. As discussed in [46, Section 1.1.1], WKB expansion is closely related to the *method* of repeated diagonalization [16, 51], both methods consisting of constructing approximate solutions from diagonal modes of a sufficiently high-order decoupled system.

*Primitive version:* We illustrate the approach by a treatment of the simplest (nonglancing) case, when  $\mu_1$  and  $\mu_2$  remain separated for all  $x \ge 0$ . This occurs, for example, on the strictly unstable set  $\Re \zeta > 0$ . Then, the decaying mode  $\mu_1$  remains separated from the remaining eigenvalues  $\mu_2, \ldots, \mu_5$  of  $G_0(x)$ . By standard matrix perturbation theory [42], it follows that there exists a change of coordinates

T, depending smoothly on  $G_0$ , such that  $T^{-1}G_0T = \begin{pmatrix} \mu_1 & 0 \\ 0 & M \end{pmatrix}$ . Making the change of coordinates  $\tilde{Z}(x) = T(x)\tilde{W}(x)$ , we convert (17) to an ODE

$$h\tilde{W}' = \begin{pmatrix} \mu_1 & 0 \\ 0 & M \end{pmatrix} \tilde{W} - hT^{-1}T'\tilde{W} + h^2T^{-1}G_1T\tilde{W}, \tag{22}$$

that, to order O(h) of the commutator term  $hT^{-1}T'$ , is block-diagonal with a decoupled  $\mu_1$  block.

Next, observe that an O(h) perturbation of a block-diagonal matrix with spectrally separated blocks may be block-diagonalized by a coordinate change  $T_2 = \mathrm{Id} + O(h)$  that is a smooth O(h) perturbation of the identity [42]; applying such a coordinate change, and observing that the associated commutator term  $hT_2^{-1}T_2' = hT_2^{-1}(O(h))' = O(h^2)$ , we can thus reduce to an equation that is block-diagonal to  $O(h^2)$ . Repeating this process, we may obtain an equation that is block-diagonal up to arbitrarily high order error  $O(h^p)$ , so long as the coefficients of the original equation (17) possess sufficient regularity that derivatives in commutator terms remain O(1).

Untangling coordinate changes, this suggests that the unique solution  $\tilde{Z}_1$  decaying as  $x \to +\infty$  "tracks" to O(h) the  $R_1$  eigendirection associated with  $\mu_1$ , satisfying the WKB-like approximation

$$\tilde{Z}_1(x) = e^{h^{-1} \int_0^x (\mu_1 + O(h))(y) dy} (R_1(x) + O(h)),$$

with in particular  $\tilde{Z}_1(0) = R_1 + O(h)$ , where  $R_1$  is an eigenvector of the decaying mode of  $-G_0^*(0^+)$ .

Recall [20, 59, 93] that the Lopatinski determinant for the component Neumann shock is

$$D_N = \ell_0 \cdot R_1,\tag{23}$$

where  $\ell_0$  is the principal part of boundary vector (18). Thus, assuming that the above approximate diagonalization procedure with formal error  $O(h^p)$  may be converted to an exact block-diagonalization with rigorous convergence error  $O(h^p)$  (as will be shown in Sect. 2.4 for any p), at least for p = 1, we may conclude that

$$D_{ZND}(\xi,\lambda) = D_N(\xi,\lambda)(1+O(h)), \tag{24}$$

where  $D_N$  is the Lopatinski determinant for the stability problem associated with the Neumann shock at x = 0, hence ZND detonation is high-frequency stable for such choices of  $\zeta$  (which include always the strictly unstable set  $\Re \zeta > 0$ ) if and only if its component Neumann shock is stable.

The glancing case. In the glancing case,  $s(x_*, \zeta_*) = 0$  for some  $x_* \ge 0$ , and there is a nontrivial turning point at  $x = x_*$ . In this case, for  $\zeta$  and x local to  $\zeta_*, x_*$ , there is no uniform separation between  $\mu_1$  and  $\mu_2$ , and the above-described complete diagonalization procedure no longer works. However, observing that  $\mu_1$  and  $\mu_2$  together remain spectrally separated from  $\mu_3, \ldots, \mu_5$ , we can still approximately

block-diagonalize to a system with coefficient  $\begin{pmatrix} P & 0 \\ 0 & N \end{pmatrix}$ , where P is a 2 × 2 block

corresponding to the total eigenspace of  $G_0$  associated with  $\mu_1$  and  $\mu_2$ , in particular having eigenvalues  $\mu_1$  and  $\mu_2$ . It is shown by a normal form analysis in [45] that any such  $2 \times 2$  block, under a nondegeneracy condition on the variation of its eigenvalues with respect to x at  $x_*$ , can be reduced further to an arbitrarily high-order perturbation  $O(h^p)$  in h of Airy's equation, written as a  $2 \times 2$  system, where in this case the nondegeneracy condition is just

$$(s^2)'(x_*) \neq 0. (25)$$

This comes from the perturbation expansion

$$\binom{0}{c(x-x_*)} \binom{1}{0} + O((x-x_*)^2) + O(h)$$
 (26)

of the associated Jordan block, where the nondegeneracy condition (25) corresponds to  $c \neq 0$ . Assuming as before that the above approximate diagonalization procedure be converted to an exact block-diagonalization with rigorous convergence error, (Sect. 2.4), at least for p=1, and that approximate Airy block (26) may be converted to an exact Airy block (shown in [45] but not treated here), we may thus hope to analyze this case by reference to the known (see, e.g., [1]) behavior of the Airy equation.

## 2.3 The Erpenbeck High-Frequency Stability Theorems

We are now ready to state our main theorems regarding profiles of the abstract system (14). We make the following assumptions:

**Assumption 2.1** The associated nonreactive system  $W_t + \sum_j \partial_{x_j} F_j(W)_x = 0$  is hyperbolic for all value of W lying on the detonation profile  $\bar{W}(x)$ .

**Assumption 2.2** The component Neumann shock for profile  $\bar{W}$  is Lopatinski stable (see discussion below (24)).

**Assumption 2.3** The coefficients of system (14) are *real analytic*.

**Definition 2.4** A detonation is type I (resp. D) if  $c_0^2 - u_1^2$  is increasing (resp. decreasing).

*Remark* 2.5 Erpenbeck classifies a number of materials/detonations as class I or D. More general cases may in principle be treated by elaboration of the techniques used to treat classes I and D.

**Theorem 2.6 (LWZ2012)** Under Assumptions 2.1, 2.2, and 2.3, plus an additional (frequently satisfied) ratio condition, type I detonations exhibit Lopatinski instabilities of arbitrarily high frequency.

Sketch of Proof (case of turning point) By the block-diagonalization procedure described above, first reduce to a  $2 \times 2$  block involving only the growth modes  $\mu_1$  and  $\mu_2$ . For type I, growth rates  $\mu_1$  and  $\mu_2$  correspond to exponentially growing/decaying modes for  $x > x_*$ , oscillatory modes for  $x < x_*$ , the connections between these solutions across the value  $x = x_*$  being determined by behavior of the Airy equation. The question is whether the Airy equation takes the pure decay mode to the corresponding pure oscillatory mode (the "decaying" mode at  $x = 0^+$ ). It does not—rather to the average of the two decaying modes [1], giving a solution composed of oscillating comparable-size parts, which, under the ratio condition,

<sup>&</sup>lt;sup>1</sup>Condition [44, (5.13)] comparing relative sizes of oscillatory modes in the first-order expansion of decaying solution  $\tilde{Z}$ , depending on the geometry of background profile  $\tilde{W}$ ; see [44, Prop. 5.1] and discussion just below.

cancel for a lattice of  $\lambda = h^{-1}i\tau + \nu$  with  $\Re \nu > 0$ . (Otherwise they cancel for frequencies  $\Re \nu < 0$  not giving instability.)

**Theorem 2.7 (LWZ2015)** Under Assumptions A1-A3, type D detonations are Lopatinski stable for sufficiently high frequencies.

Sketch of Proof (case of turning point) As in case I, the problem reduces to a  $2 \times 2$  block, and the study of connections across the turning point  $x = x_*$  determined by behavior of the Airy equation. For type D, the reverse happens, By reflection symmetry of the Airy equation, there holds in case D essentially the reverse situation to that of case I, featuring oscillatory modes for  $x > x_*$  and exponentially growing/decaying modes for  $x < x_*$ , connected by a reverse Airy flow. So, again we see that the pure "decay" (now actually oscillating) mode at  $+\infty$  does not connect to the pure growth mode at  $x = x_*$ , but contains at least some component of the (actual) "decay" mode for  $x < x_*$ . It follows by order  $e^{O(x/h)}$  exponential growth in the backward direction of this decaying mode, together with order  $e^{O(-x/h)}$  exponential decay in the backward direction of the complementary growing mode, that the solution at x = 0 is dominated by the decay-mode component Thus,  $\tilde{Z}(0^+)$  lies to exponentially small order in the  $R_1$  direction,  $R_1$  as in (23), giving the (stable) shock Lopatinski determinant in the limit, as in the simplest (nonglancing) case.

Technical issues: 1. Exact vs. approximate block-diagonalization. 2. Block-diagonalization at  $+\infty$ . 3. Turning points at  $x_* = 0, +\infty$ , and exact vs. approximate conjugation to Airy/Bessel (daunting). Issues 1 and 2 are resolved below; issue 3 (not treated here) is resolved in [45].

*Remark* 2.8 1. Theorems 2.6 and 2.7 give rigorous justification of numerical multid stability stability computations for ZND, several aspects of which were previously unclear [78].

- 2. The arguments streamline/modernize the analysis of [22, 23] (carried out originally by WKB expansion in all 5 modes!). But also new analysis at degenerate frequencies is needed for the complete stability result.<sup>2</sup>
- 3. The proofs are still hard work! (Amazing achievement of Erpenbeck in the 1960s.)
- 4. We have suppressed discussion of conjugations to Airy/Bessel equations (difficult! the latter new), and related huge contributions of Olver and others in asymptotics of special functions [1, 65].

<sup>&</sup>lt;sup>2</sup> As discussed in [45], Erpenbeck treated turning points/glancing modes at points  $x_*$  bounded away from 0 and  $\infty$ ; however, these cases necessarily occur at certain boundary frequencies, so must be considered in a complete stability analysis, as must be issues not treated in [22] of uniformity for frequencies near but not at a glancing point.

## 2.4 Exact Block-Diagonalization and $C^{\infty}$ vs. $C^{\omega}$ Stationary Phase

(Following [46]) Consider an approximately block-diagonal equation

$$hW' = AW + h^p \Theta,$$

$$A = \begin{pmatrix} A_{11} & 0 \\ 0 & A_{22} \end{pmatrix}$$
,  $\Theta = \text{error}$ , and seek  $T = \begin{pmatrix} I & h^p \alpha_{12} \\ h^p \alpha_{21} & I \end{pmatrix}$  such that  $W = TZ$  gives an exact conjugation to  $hZ' = DZ$ , with  $D$  diagonal, accuracy  $p = 1$  being sufficient for our stability arguments. Equating first diagonal, then off-diagonal blocks in  $(hT' + TD)Z = (A + h^p \Theta)TZ$ , yields Ricatti equations

$$h\alpha'_{12} = A_{11}\alpha_{12} - \alpha_{12}A_{22} + \Theta_{12} - h^{2p}\alpha_{12}\Theta_{21}\alpha_{21} - h^{p}\Theta_{11}\alpha_{21},$$
  

$$h\alpha'_{21} = A_{22}\alpha_{21} - \alpha_{21}A_{11} + \Theta_{21} - h^{2p}\alpha_{21}\Theta_{12}\alpha_{12} - h^{p}\Theta_{22}\alpha_{21},$$
(27)

or, viewed as a block vector equation in  $\alpha = (\alpha_{12}, \alpha_{21})$ :

$$h\alpha' = \mathcal{A}(0)\alpha + (\mathcal{A}(z) - \mathcal{A}(0))\alpha + Q(\alpha, \Theta, h). \tag{28}$$

Observation Sylvester equation, hence  $\sigma(A_{11}) \cap \sigma(A_{22}) = \emptyset$  implies  $0 \notin \sigma(\mathcal{A}(0))$ .

## 2.4.1 Lyapunov-Perron Formulation (Standard)

From  $h\alpha' = \mathcal{A}(0)\alpha + (\mathcal{A}(z) - \mathcal{A}(0))\alpha + Q(\alpha, \Theta, h)$ , we obtain by Duhamel's principle the integral fixed-point equation

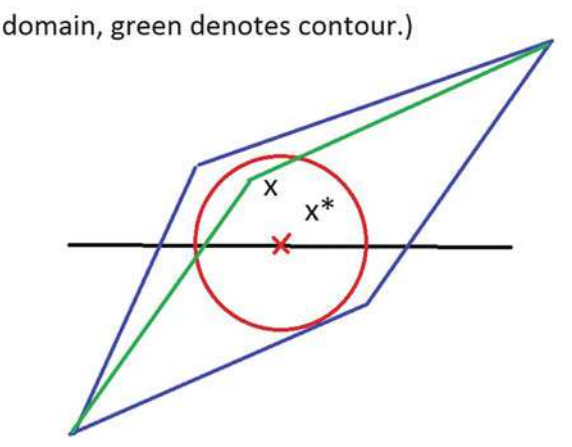
$$\alpha(x) = \mathcal{T}\alpha(x) := h^{-1} \int_{z_*}^x e^{h^{-1} \mathcal{A}(0)(x-y)} \Pi_S ((\mathcal{A}(y) - \mathcal{A}(0))\alpha(y) + Q(y)) dy + h^{-1} \int_{z_*}^x e^{h^{-1} \mathcal{A}(0)(x-y)} \Pi_U ((\mathcal{A}(y) - \mathcal{A}(0))\alpha(y) + Q(y)) dy,$$
(29)

on diamond  $\mathcal{D} := \{x : |\arg((x-z_*)/\gamma)|, |\arg((z^*-x)/\gamma)| \le \varepsilon\}$ , where  $\gamma \in \mathbb{C}$ ,  $|\gamma| = 1$  is chosen so that  $\mathcal{A}(0)\gamma$  has spectral gap, and  $\Pi_U$ ,  $\Pi_S$  denote stable/unstable projectors of  $\mathcal{A}(0)\gamma$ ; see Fig. 8. Mapping  $\mathcal{T}$  is contractive by  $O(e^{-\eta|x-y|/h})$  decay of propagators, plus smallness of the source.

Remark 2.9 Here, we have used analyticity to escape the real axis and recover a spectral gap. This is essentially a finite-regularity version of a theorem of Wasow [85] in the h-analytic case [46].

Fig. 8 Block diagonalization at a finite point

Diagonalization at a finite point. (Blue encloses



## 2.4.2 Block Diagonalization at Infinity

In many problems (e.g., detonation), we must treat unbounded intervals, diagonalization at infinity. A bit of thought shows that the finite-domain fixed-point construction of (29), depicted in Fig. 8, does not work:on the infinite domain, for the reason that points  $z^*$ ,  $z_*$  would have to run out to infinity in  $\pm \gamma$  directions in order to accomodate x on an interval  $(M, \infty)$  on the real axis, hence the domain  $\mathcal D$  would become a half-space and the integrals of (29) no longer necessarily converge (nor even b: defined, since ODE coefficients would not necessarily extend). We treat this case instead by the following modifications of the argument for the finite-turning point case [46]. Briefly, we:

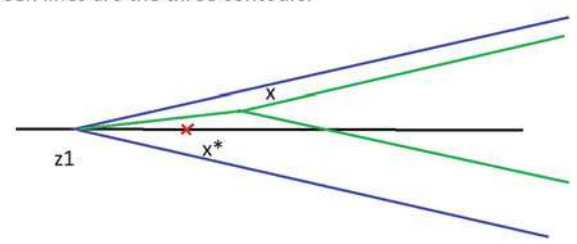
- Require analyticity on a wedge about infinity, not just a neighborhood of the real axis, with exponential decay as  $\Re z \to \infty$  (and verify that this is indeed guaranteed by stable manifold construction for an analytic coefficient profile equation).
- Use three contour directions to recover a spectral gap, while restricting the fixed-point domain  $\mathcal{D}$  to the wedge of analyticity of coefficients (with convergence of integrals coming partly from exponential decay of  $(\mathcal{A}(y) \mathcal{A}(\infty))$ , replacing smallness |y| << 1 i: the finite case); see Fig. 9.

## 2.5 Counterexamples and $C^{\infty}$ vs. $C^{\omega}$ Stationary Phase

Our treatment of multi-D high-frequency behavior has a different flavor from the analyses of 1-D stability in part one: in particular, we have used analyticity of coefficients and moved away from the real line.

Fig. 9 Block diagonalization at infinity: contour configuration

Exact diagonalization at infinity. Blue wedge is domain, green lines are the three contours.



A natural question: Is this necessary? In particular, could we by some other method perform block-diagonalization for  $C^{\infty}$  (or just  $C^r$  as in the 1-D case) coefficients? *Rephrasing:* 1. Is a spectral gap between blocks (as in classical ODE techniques [50]) needed for exact  $C^{\infty}$  diagonalization, or just spectral separation? (Here, we define spectral gap between eigenvalues as nonzero real part and spectral separation as nonzero modulus of their difference.) And, 2. (Wasow, 1980s [85]) Can analytic block-diagonalization be performed globally under appropriate global assumptions?

### 2.5.1 Counterexamples: Reduction to Oscillatory Integral

The answers to the above questions are "yes" (spectral gap is needed) and "no" [46], as we now describe. Consider the  $2 \times 2$  triangular system

$$hW' = \mathcal{A}(x,h)W := \begin{pmatrix} \lambda_1(x) & h^p \theta(x) \\ 0 & \lambda_2(x) \end{pmatrix} W, \qquad W \in \mathbb{C}^2, \ p \ge 1, \tag{30}$$

 $\theta$  uniformly bounded, with globally separated eigenvalues  $\lambda_1(x) = x + i$ ,  $\lambda_2 = -(x + i)$ .

**Lemma 2.10** ([46]) There exists T(x,h) on  $[-L,L] \subset \mathbb{R}$ ,  $0 \le h \le h_0$ , T,  $T^{-1}$  uniformly bounded in  $C^1$ , for which W = TZ converts (30) to a diagonal system hZ' = D(x,h)Z, if and only if

$$\int_{-x}^{x} e^{-y^2/h - 2iy/h} \theta(y) dy \lesssim h e^{-x^2/h} \text{ for all } |x| \leq L.$$
 (31)

Sketch of proof It is sufficient to seek a triangular diagonalizer  $T = \begin{pmatrix} 1 & h^p \alpha \\ 0 & 1 \end{pmatrix}$ , in which case Ricatti equation (27) reduces to a scalar, linear ODE in  $\alpha$ :

$$h\alpha' = (\lambda_1 - \lambda_2)\alpha + \theta. \tag{32}$$

By Duhamel's principle/variation of constants, existence of a uniformly bounded *T* thus implies uniform boundedness of

$$\alpha(x,h) = h^{-1} \int_0^x e^{h^{-1} \int_y^x (\lambda_1 - \lambda_2)(z) dz} \theta(y) dy - e^{h^{-1} \int_0^x (\lambda_1 - \lambda_2)(z) dz} \alpha(0,h)$$

$$= e^{(x^2 + 2ix)/h} \left( h^{-1} \int_0^x e^{-(y^2 + 2iy)/h} \theta(y) dy - \alpha(0,h) \right).$$

The direction ( $\Leftarrow$ ) then follows by  $e^{-2ix}\alpha(x) - e^{2ix}\alpha(-x) = e^{x^2/h} \int_{-x}^x e^{-(y^2 + 2iy)/h} \theta(y) dy$ .

The direction ( $\Rightarrow$ ) follows by direct computation, choosing  $\alpha(0,h) = h^{-1} \int_0^L e^{-(y^2+2iy)/h} \theta(y) dy$ .

### 2.5.2 Failure of Global Conjugators

**Lemma 2.11** ([46]) For  $a \not\equiv 0$  analytic on  $[-L, L] \times [-i, i]$ , and  $h \rightarrow 0^+$ ,

$$\int_{-x}^{x} e^{-y^{2}/h - 2iy/h} a(y) dy \begin{cases} \lesssim h e^{-\frac{x^{2}}{h}}, & 0 < x \le L < 1, \\ \sim h^{(j+1)/2} e^{-\frac{1}{h}}, & 1 < c_{0} \le x \le L, \end{cases}$$
(33)

where j = order of first nonvanishing derivative of a at z = i.

*Proof* The general case follows by complex-analytic stationary phase estimates (see [56, 67]). The simplest case  $a \equiv 1$  (enough for a counterexample), follows from  $\int_{-\infty}^{+\infty} e^{-y^2/h-2iy/h} dy = e^{-1/h}$ , which follows from the fact that the Fourier transform of a Gaussian is Gaussian.

Consequence: Lemma 2.11 implies that there is no bounded block-diagonalizing conjugator of (30) on [-x, x] for |x| > 1, resolving a 30-year open question of Wasow [85].

## 2.5.3 Failure of Local Conjugators for $C^{\infty}$ Coefficients

**Lemma 2.12** ([46]) For  $0 < c_0 \le x$  and  $a(y) := e^{-y^{-1/(s-1)}}$  for y > 0 and 0 for  $y \le 0$ ,

$$\int_{-x}^{x} e^{-y^2/h - 2iy/h} a(y) dy \sim h^{1 - 1/2s} e^{\frac{-c(s) + d(s)h^{1 - 1/s} + O(h^{2(1 - 1/s)})}{h^{1/s}}},$$

 $1 < s < \infty$ , as  $h \to 0^+$ , for any x > 0, where c(s) > 0, and  $\Re d(s) < 0$  for s < 2.

*Proof (Sketch of proof)* Defining  $\alpha=1-1/s\in(0,1), \beta=e^{-\frac{i\pi(1-1/s)}{2}}$ , deform contour  $[0,+\infty]$  to  $z=h^{\alpha}\beta t, t\in(0,+\infty)$ , to obtain  $I(h)\sim h^{\alpha}\int_{0}^{\infty}e^{\frac{i\beta(-2t-t^{-\theta}+i\beta h^{\alpha}t^{2})}{h^{1-\alpha}}}dt$ , then apply a standard stationary phase estimate about the nondegenerate maximum of the phase at  $t_{0}=2^{-(1-1/s)}+O(h)$ .

Consequence: Lemma 2.12 implies that there is no bounded block-diagonalizing conjugator of (30) on [-x, x] for |x| > 0, resolving question 1 of Sect. 2.5 (Taking  $\theta(y)$  to be the symbol a(y) of Lemma 2.12 gives  $\int_{-x}^{x} e^{-y^2/h - 2iy/h} \theta(y) dy \sim$ 

$$h^{1-1/2s}e^{\frac{-c(s)}{h^{1/s}}} \gg he^{-x^2/h}$$
 for any  $x > 0$ ,  $s > 1$ .)

*Moral:* Results may vary for  $C^{\infty}$  coefficients!

Related phenomena: 1. Different qualitative nature of diffraction by  $C^{\infty}$  vs. analytic boundary in  $\mathbb{R}^3$  G. Lebeau, Private communication. 2. Instability of analytic-coefficient spectra under  $C^{\infty}$  perturbations: probability one of a Weyl distribution ("cloud") for asymptotic spectrum of a random  $C^{\infty}$ -perturbation of an analytic-coefficient operator with asymptotic spectra initially confined to a curve [31].

## 2.5.4 Coda: Gevrey-Regularity Stationary Phase

For Gevrey norm  $||a||_{s,T} := \sup_j |\partial_x^j a|(j!)^s/T^j$ , define the Gevrey class  $\mathcal{G}^{s,T}$  of functions with bounded Gevrey norm. Here, s=1 corresponds to analyticity on a strip of width T about the real axis  $\mathbb{R}$ , while  $s \to \infty$  corresponds to absence of regularity, with Gevrey-class functions interpolating between. The following result gives an upper bound corresponding to the lower bound of Lemma 2.12.

**Proposition 2.13** ([46]) For  $a \in \mathcal{G}^{s,T_0}$  on [-L,L],  $T_0,T > 1$ ,  $|x| \leq L$ , and some  $c = c(T_1,T,s) > 0$ ,

$$\int_{-x}^{x} e^{-y^2/h - 2iy/h} a(y) dy \lesssim h^{1/2} ||a||_{T,s} e^{-c/h^{1/s}}.$$
 (34)

Proposition 2.13 interpolates between the algebraic  $O(h^r)$  van der Korput bounds for  $C^r$  symbols (roughly,  $s = \infty$ ) and the exponential  $O(h^{1/2}e^{-1/h})$  bounds for analytic symbols a obtained by the saddlepoint method/analytic stationary phase. Lemma 2.12 shows that (34) is sharp.

(Proof by Fourier cutoff/standard complex-analytic stationary phase.)

## 2.6 Discussion and Open Problems

Our turning-point analyses in the first part of this section completes and somewhat simplifies the high-frequency stability program laid out by Erpenbeck in the 1960s, in his tour de force analyses [22, 23]. This in turn solidifies the foundation of the

many (and delicate) numerical multi-D stability studies for ZND, by rigorously truncating the computational frequency domain. On the other hand, our analysis in the second part of this section on sensitivity of block-diagonalization/WKB expansion with respect to  $C^{\infty}$  (indeed, Gevrey-class) perturbations raises interesting philosophical questions about the physical meaning of our multi-D high-frequency stability results, as intuitively we think of physical coefficients as inexactly known.

Recall that the 1-D high-frequency stability results of [91] used a different, C' diagonalization method, so this issue does not arise in 1-D. Likewise, smooth dependence on coefficients with respect to  $C^r$  perturbation of the Evans-Lopatinski determinant  $D_{ZND}(\xi,\lambda)$  restricted to compact frequency domains [68] implies that the *strict instabilities* asserted for analytic coefficients in Theorem 2.6 persist under  $C^r$  perturbations of the coefficients, so there is no issue for our instability results. That is, the Evans function is itself robust, independent of the methods that we used to estimate it. Even in the stable case, we obtain from this point of view robust stability estimates on any bounded domain, no matter how large, in particular for domains far out of practical computation range. Thus, the results of Theorem 2.7 have practical relevance in this restricted sense independent of questions regarding analyticity of coefficients. The philosophical resolution of the remaining issue for ultra-high frequencies, may perhaps, similarly as other issues touched on in Sect. 1, lie in the inclusion of transport (viscosity/heat conduction/diffusion) effects, which stabilize spectrum for frequencies on the order of one over the size of associated coefficients.

## Open problems:

- ZND limit for multi-d (interaction of viscosity, turning points).
- Multi-d numerics for rNS (no apparent obstacle, but computationally intensive).
- Rigorous analysis of 1-d viscous hyperstabilization (again, apparent interaction of turning points vs. viscous effects).

**Acknowledgements** Special thanks to the anonymous and extraordinarily attentive referee, whose many thoughtful suggestions and comments greatly improved the exposition.

## References

- M. Abramowitz, I.A. Stegun, Handbook of Mathematical Functions with Formulas, Graphs, and Mathematical Tables. National Bureau of Standards Applied Mathematics Series, vol. 55
   For sale by the Superintendent of Documents (U.S. Government Printing Office, Washington DC, 1964), xiv+1046pp.
- J. Alexander, R. Gardner, C. Jones, A topological invariant arising in the stability analysis of travelling waves. J. Reine Angew. Math. 410, 167–212 (1990)
- S. Alinhac, Existence d'ondes de raréfaction pour des systèmes quasi-linéaires hyperboliques multidimensionnels (French) [Existence of rarefaction waves for multidimensional hyperbolic quasilinear systems]. Commun. Partial Differ. Equ. 14(2), 173–230 (1989)
- 4. B. Barker, J. Humpherys, K. Zumbrun, STABLAB: a MATLAB-based numerical library for Evans function computation (2015). Available at: http://impact.byu.edu/stablab/

- 5. B. Barker, J. Humpherys, G. Lyng, K. Zumbrun, Viscous hyperstabilization of detonation waves in one space dimension. SIAM J. Appl. Math. **75**(3), 885–906 (2015)
- B. Barker, K. Zumbrun, A numerical investigation of stability of ZND detonations for Majda's model, preprint. arxiv:1011.1561
- 7. B. Barker K. Zumbrun, Numerical stability of ZND detonations, in preparation
- 8. G. K. Batchelor. *An Introduction to Fluid Dynamics*, paperback edn. Cambridge Mathematical Library (Cambridge University Press, Cambridge, 1999)
- 9. M. Beck, B. Sandstede, K. Zumbrun, Nonlinear stability of time-periodic viscous shocks. Arch. Ration. Mech. Anal. **196**(3), 1011–1076 (2010)
- A. Bourlioux, A. Majda, V. Roytburd, Theoretical and numerical structure for unstable onedimensional detonations. SIAM J. Appl. Math. 51, 303–343 (1991)
- 11. L.Q. Brin, Numerical testing of the stability of viscous shock waves. Math. Comput. **70**(235), 1071–1088 (2001)
- 12. J. Buckmaster, The contribution of asymptotics to combustion. Phys. D 20(1), 91–108 (1986)
- J. Buckmaster, J. Neves, One-dimensional detonation stability: the spectrum for infinite activation energy. Phys. Fluids 31(12), 3572–3576 (1988)
- D.L. Chapman, VI. On the rate of explosion in gases. Philos. Mag. Ser. 5 47(284), 90–104 (1899). doi:10.1080/14786449908621243
- P. Clavin, L. He, Stability and nonlinear dynamics of one-dimensional overdriven detonations in gases. J. Fluid Mech. 306, 306–353 (1996)
- E.A. Coddington, M. Levinson, Theory of Ordinary Differential Equations (McGraw-Hill Book Company, Inc., New York, 1955)
- 17. R. Courant, K.O. Friedrichs, *Supersonic Flow and Shock Waves* (Springer-Verlag, New York, 1976), xvi+464pp.
- 18. W. Döring, Über Detonationsvorgang in Gasen [On the detonation process in gases]. Ann. Phys. 43, 421–436 (1943). doi:10.1002/andp.19434350605
- J.J. Erpenbeck, Stability of steady-state equilibrium detonations. Phys. Fluids 5, 604–614 (1962)
- 20. J.J. Erpenbeck, Stability of step shocks. Phys. Fluids **5**(10), 1181–1187 (1962)
- 21. J.J. Erpenbeck, Stability of idealized one-reaction detonations. Phys. Fluids 7, 684 (1964)
- 22. J.J. Erpenbeck, Stability of Detonations for Disturbances of Small Transverse Wave-Length Los Alamos, LA-3306 (1965), 136pp. https://www.google.com/search?tbm=bks&hl=en& q=Stability+of+detonation+for+disturbances+of+small+transverse+wavelength+Report+of+ los+Alamos+LA3306+1965
- J.J. Erpenbeck, Detonation stability for disturbances of small transverse wave length. Phys. Fluids 9, 1293–1306 (1966)
- 24. L.M. Faria, A.R. Kasimov, R.R. Rosales, Study of a model equation in detonation theory. SIAM J. Appl. Math. 74(2), 547–570 (2014)
- W. Fickett, W.C. Davis, *Detonation* (University of California Press, Berkeley, 1979); reissued as *Detonation: Theory and Experiment* (Dover Press, Mineola, New York 2000). ISBN:0-486-41456-6
- W. Fickett, W. Wood, Flow calculations for pulsating one-dimensional detonations. Phys. Fluids 9, 903–916 (1966)
- R.A. Gardner, K. Zumbrun, The gap lemma and geometric criteria for instability of viscous shock profiles. Commun. Pure Appl. Math. 51(7), 797–855 (1998)
- I. Gasser, P. Szmolyan, A geometric singular perturbation analysis of detonation and deflagration waves. SIAM J. Math. Anal. 24, 968–986 (1993)
- O. Gues, G. Métivier, M. Williams, K. Zumbrun, Existence and stability of multidimensional shock fronts in the vanishing viscosity limit. Arch. Ration. Mech. Anal. 175(2), 151–244 (2005)
- O. Gues, G. Métivier, M. Williams, K. Zumbrun, Existence and stability of noncharacteristic boundary layers for the compressible Navier-Stokes and MHD equations. Arch. Ration. Mech. Anal. 197(1), 1–87 (2010)

31. M. Hager, J. Sjöstrand, Eigenvalue asymptotics for randomly perturbed non-selfadjoint operators. Math. Ann. **342**(1), 177–243 (2008)

- 32. J. Hendricks, J. Humpherys, G. Lyng, K. Zumbrun, Stability of viscous weak detonation waves for Majda's model. J. Dyn. Differ. Equ. 27(2), 237–260 (2015)
- J. Humpherys, G. Lyng, K. Zumbrun, Multidimensional spectral stability of large-amplitude Navier-Stokes shocks, preprint. arxiv:1603.03955
- 34. J. Humpherys, K. Zumbrun, An efficient shooting algorithm for Evans function calculations in large systems. Physica D **220**(2), 116–126 (2006)
- 35. J. Humpherys, G. Lyng, K. Zumbrun, Spectral stability of ideal gas shock layers. Arch. Ration. Mech. Anal. **194**(3), 1029–1079 (2009)
- 36. J. Humpherys, O. Lafitte, K. Zumbrun, Stability of isentropic Navier-Stokes shocks in the high-Mach number limit. Commun. Math. Phys. **293**(1), 1–36 (2010)
- J. Humpherys, K. Zumbrun, Efficient numerical stability analysis of detonation waves in ZND.
   Q. Appl. Math. 70(4), 685–703 (2012)
- 38. E. Jouguet, Sur la propagation des réactions chimiques dans les gaz [On the propagation of chemical reactions in gases]. J. Math. Pures Appl. 6(1), 347–425 (1905)
- E. Jouguet, Sur la propagation des réactions chimiques dans les gaz [On the propagation of chemical reactions in gases]. J. Math. Pures Appl. 6(2), 5–85 (1906)
- H.K. Jenssen, G. Lyng, M. Williams, Equivalence of low-frequency stability conditions for multidimensional detonations in three models of combustion. Indiana Univ. Math. J. 54, 1–64 (2005)
- A.R. Kasimov, D.S. Stewart, Spinning instability of gaseous detonations. J. Fluid Mech. 466, 179–203 (2002)
- 42. T. Kato, Perturbation Theory for Linear Operators (Springer, Berlin, 1985)
- 43. H.O. Kreiss, Initial boundary value problems for hyperbolic systems. Commun. Pure Appl. Math. 23, 277–298 (1970)
- O. Lafitte, M. Williams, K. Zumbrun, The Erpenbeck high frequency instability theorem for Zeldovitch-von Neumann-Döring detonations. Arch. Ration. Mech. Anal. 204(1), 141–187 (2012)
- O. Lafitte, M. Williams, K. Zumbrun, High-frequency stability of detonations and turning points at infinity. SIAM J. Math. Anal. 47(3), 1800–1878 (2015)
- 46. O. Lafitte, M. Williams, K. Zumbrun, Block-diagonalization of ODEs in the semiclassical limit and  $C^{\omega}$  vs.  $C^{\infty}$  stationary phase. SIAM J. Math. Anal. **48**(3), 1773–1797 (2016)
- P.D. Lax, Hyperbolic systems of conservation laws. II. Commun. Pure Appl. Math. 10, 537– 566 (1957)
- 48. P.D. Lax, Hyperbolic Systems of Conservation Laws and the Mathematical Theory of Shock Waves. Conference Board of the Mathematical Sciences Regional Conference Series in Applied Mathematics, vol. 11 (Society for Industrial and Applied Mathematics, Philadelphia, 1973), v+48pp.
- 49. H.I. Lee, D.S. Stewart, Calculation of linear detonation instability: one-dimensional instability of plane detonation. J. Fluid Mech. **216**, 103–132 (1990)
- J.H.S. Lee, *The Detonation Phenomenon* (Cambridge University Press, Cambridge/New York, 2008). ISBN-13:978-0521897235
- 51. N. Levinson, The asymptotic nature of solutions of linear systems of differential equations. Duke Math. J. 15, 111–126 (1948)
- 52. T.-P. Liu, S.-H. Yu, Nonlinear stability of weak detonation waves for a combustion model. Commun. Math. Phys. **204**(3), 551–586 (1999)
- 53. G. Lyng, K. Zumbrun, One-dimensional stability of viscous strong detonation waves. Arch. Ration. Mech. Anal. 173(2), 213–277 (2004)
- 54. G. Lyng, K. Zumbrun, A stability index for detonation waves in Majda's model for reacting flow. Physica D **194**, 1–29 (2004)
- G. Lyng, M. Raoofi, B. Texier, K. Zumbrun, Pointwise Green function bounds and stability of combustion waves. J. Differ. Equ. 233, 654

  –698 (2007)

- A. Martinez, An Introduction to Semiclassical and Microlocal Analysis (Springer, New York, 2002)
- G. Métivier, K. Zumbrun, Large viscous boundary layers for noncharacteristic nonlinear hyperbolic problems. Mem. Am. Math. Soc. 175(826), vi+107pp (2005)
- 58. A. Majda, A qualitative model for dynamic combustion. SIAM J. Appl. Math. 41, 70–91 (1981)
- 59. A. Majda, The stability of multi-dimensional shock fronts a new problem for linear hyperbolic equations. Mem. Am. Math. Soc. 275, 1–95 (1983)
- 60. A. Majda, R. Rosales, A theory for spontaneous Mach stem formation in reacting shock fronts. I. The basic perturbation analysis. SIAM J. Appl. Math. 43, 1310–1334 (1983)
- C. Mascia, K. Zumbrun, Pointwise Green's function bounds for shock profiles with degenerate viscosity. Arch. Ration. Mech. Anal. 169, 177–263 (2003)
- 62. G. Métivier, The block structure condition for symmetric hyperbolic problems. Bull. Lond. Math. Soc. 32, 689–702 (2000)
- 63. G. Métivier, Stability of multidimensional shocks, in *Advances in the Theory of Shock Waves*. Progress in Nonlinear Differential Equations and Applications, vol. 47 (Birkhäuser Boston, Boston, 2001), pp. 25–103
- T. Nguyen, Stability of multi-dimensional viscous shocks for symmetric systems with variable multiplicities. Duke Math. J. 150(3), 577–614 (2009)
- 65. F.W.U. Olver, Asymptotics and Special Functions (Academic Press, New York, 1974)
- R. L. Pego, M. I. Weinstein, Eigenvalues, and instabilities of solitary waves. Philos. Trans. R. Soc. Lond. Ser. A 340(1656), 47–94 (1992)
- 67. R. Pemantle, M.C. Wilson, Asymptotic expansions of oscillatory integrals with complex phase, in *Algorithmic Probability and Combinatorics*. Contemporary Mathematics, vol. 520 (American Mathematical Society, Providence, 2010), pp. 221–240
- 68. R. Plaza, K. Zumbrun, An Evans function approach to spectral stability of small-amplitude shock profiles. J. Discret. Cont. Dyn. Sys. 10, 885–924 (2004)
- 69. J.M. Powers, S. Paolucci, Accurate spatial resolution estimates for reactive supersonic flow with detailed chemistry. AIAA J. 43(5), 1088–1099 (2005)
- C.M. Romick, T.D. Aslam, J.D. Powers, *The Dynamics of Unsteady Detonation with Diffusion*.
   49th AIAA Aerospace Sciences Meeting including the New Horizons Forum and Aerospace Exposition, Orlando (2011), http://dx.doi.org/10.2514/6.2011-799
- C.M. Romick, T.D. Aslam, J.D. Powers, The effect of diffusion on the dynamics of unsteady detonations. J. Fluid Mech. 699, 453–464 (2012)
- J.-M. Roquejoffre, J.-P. Vila, Stability of ZND detonation waves in the Majda combustion model. Asymptot. Anal. 18(3–4), 329–348 (1998)
- B. Sandstede, A. Scheel, Hopf bifurcation from viscous shock waves. SIAM J. Math. Anal. 39, 2033–2052 (2008)
- 74. D. Serre, *Systèmes de lois de conservation I–II* (Fondations, Diderot Editeur, Paris, 1996), iv+308pp. ISBN:2-84134-072-4 and xii+300pp. ISBN:2-84134-068-6
- 75. M. Short, An Asymptotic Derivation of the Linear Stability of the Square-Wave Detonation using the Newtonian limit. Proc. R. Soc. Lond. A **452**, 2203–2224 (1996)
- M. Short, Multidimensional linear stability of a detonation wave at high activation energy. SIAM J. Appl. Math. 57(2), 307–326 (1997)
- 77. J. Smoller, Shock Waves and Reaction–Diffusion Equations, 2nd edn. Grundlehren der Mathematischen Wissenschaften, Fundamental Principles of Mathematical Sciences, vol. 258 (Springer, New York, 1994), xxiv+632pp. ISBN:0-387-94259-9
- 78. D.S. Stewart, A.R. Kasimov, State of detonation stability theory and its application to propulsion. J. Propuls. Power **22**(6), 1230–1244 (2006)
- A. Szepessy, Dynamics and stability of a weak detonation wave. Commun. Math. Phys. 202(3), 547–569 (1999)
- B. Texier, K. Zumbrun, Galloping instability of viscous shock waves. Physica D. 237, 1553– 1601 (2008)
- B. Texier, K. Zumbrun, Hopf bifurcation of viscous shock waves in gas dynamics and MHD. Arch. Ration. Mech. Anal. 190, 107–140 (2008)

- 82. B. Texier, K. Zumbrun, Transition to longitudinal instability of detonation waves is generically associated with Hopf bifurcation to time-periodic galloping solutions. Commun. Math. Phys. **302**(1), 1–51 (2011)
- 83. J. von Neumann, *Theory of Detonation Waves*, Aberdeen Proving Ground, Maryland: Office of Scientific Research and Development, Report No. 549, Ballistic Research Laboratory File No. X-122 Progress Report to the National Defense Research Committee, Division B, OSRD-549 (April 1, 1942. PB 31090). (4 May 1942), 34 pages
- 84. J. von Neumann, in *John von Neumann, Collected Works*, vol. 6. ed. by A.J. Taub (Permagon Press, Elmsford, 1963) [1942], pp. 178–218
- 85. W. Wasow, *Linear Turning Point Theory*. Applied Mathematical Sciences, vol. 54 (Springer-Verlag, New York, 1985), ix+246pp.
- M. Williams, Heteroclinic orbits with fast transitions: a new construction of detonation profiles. Indiana Univ. Math. J. 59(3), 1145–1209 (2010)
- 87. Y.B. Zel'dovich, [On the theory of the propagation of detonation in gaseous systems]. J. Exp. Theor. Phys. **10**, 542–568 (1940). Translated into English in: National Advisory Committee for Aeronautics Technical Memorandum No. 1261 (1950)
- 88. K. Zumbrun, Multidimensional stability of planar viscous shock waves, in *Advances in the Theory of Shock Waves*. Progress in Nonlinear Differential Equations and Applications, vol. 47 (Birkhäuser Boston, Boston, 2001), pp. 307–516
- 89. K. Zumbrun, Stability of large-amplitude shock waves of compressible navier–stokes equations, with an appendix by Helge Kristian Jenssen and Gregory Lyng, in *Handbook of Mathematical Fluid Dynamics*, vol. III (North-Holland, Amsterdam, 2004), pp. 311–533
- K. Zumbrun, Stability of detonation waves in the ZND limit. Arch. Ration. Mech. Anal. 200(1), 141–182 (2011)
- 91. K. Zumbrun, High-frequency asymptotics and one-dimensional stability of Zel'dovich-von Neumann-Döring detonations in the small-heat release and high-overdrive limits. Arch. Ration. Mech. Anal. **203**(3), 701–717 (2012)
- 92. K. Zumbrun, P. Howard, Pointwise semigroup methods and stability of viscous shock waves. Indiana Math. J. 47, 741–871 (1998); Errata, Indiana Univ. Math. J. 51(4), 1017–1021 (2002)
- 93. K. Zumbrun, D. Serre, Viscous and inviscid stability of multidimensional planar shock fronts. Indiana Univ. Math. J. **48**, 937–992 (1999)